Offline and Online Adaboost for Detecting Anatomic Structures

by

Hong Wu

A Thesis Presented in Partial Fulfillment
of the Requirements for the Degree
Master of Science

Approved July 2011 by the
Graduate Supervisory Committee:

Jianming Liang, Chair
Gerald Farin
Jieping Ye

ARIZONA STATE UNIVERSITY

August 2011

ABSTRACT

Detecting anatomical structures, such as the carina, the pulmonary trunk and the aortic arch, is an important step in designing a CAD system of detection Pulmonary Embolism.

The presented CAD system gets rid of the high-level prior defined knowledge to become a system which can easily extend to detect other anatomic structures. The system is based on a machine learning algorithm — AdaBoost and a general feature — Haar. This study emphasizes on off-line and on-line AdaBoost learning. And in on-line AdaBoost, the thesis further deals with extremely imbalanced condition.

The thesis first reviews several knowledge-based detection methods, which are relied on human being's understanding of the relationship between anatomic structures. Then the thesis introduces a classic off-line AdaBoost learning. The thesis applies different cascading scheme, namely multi-exit cascading scheme. The comparison between the two methods will be provided and discussed.

Both of the off-line AdaBoost methods have problems in memory usage and time consuming. Off-line AdaBoost methods need to store all the training samples and the dataset need to be set before training. The dataset cannot be enlarged dynamically. Different training dataset requires retraining the whole process. The retraining is very time consuming and even not realistic.

To deal with the shortcomings of off-line learning, the study exploited on-line AdaBoost learning approach. The thesis proposed a novel pool based on-line method with Kalman filters and histogram to better represent the distribution of the samples' weight. Analysis of the performance, the stability and the computational complexity will be provided in the thesis.

Furthermore, the original on-line AdaBoost performs badly in imbalanced conditions, which occur frequently in medical image processing. In image dataset, positive samples are limited and negative samples are countless. A novel Self-Adaptive Asymmetric On-line Boosting method is presented. The method utilized a new asymmetric loss criterion with self-adaptability according to the ratio of exposed positive and negative samples and it has an advanced rule to update sample's importance weight taking account of both classification result and sample's label. Compared to traditional on-line AdaBoost Learning method, the new method can achieve far more accuracy in imbalanced conditions.

DEDICATION

Dedicated the work to my family

ACKNOWLEDGEMENTS

I would like to thank my advisor, Dr. Jianming Liang, for his continued and patient guidance during the study of the whole Master degree. Dr. Liang's vision and construction criticisms have helped me accomplish my goals.

Special thanks to Deng Kun, Nima Tajbakhsh and Wenzhe Xue for helping me during the various stages of my researchs.

My deepest gratitude to my family's constant help.

TABLE OF CONTENTS

LIST OF TABLES

LIST OF FIGURES

Chapter 1

INTRODUCTION

CT pulmonary angiography (CTPA) has been widely used in diagnosis. Due to the high volume of the data, human error and fatigue, interpreting the images manually is complex and time consuming. Many computer aided diagnosis (CAD) [1, 2, 3, 4] systems have been proposed for different purposes. In the thesis, we focus on the task of identification of anatomical structures to assist the diagnosis.

1.1 Background

Our long-term goal is to develop a high-performance computer aided diagnosis (CAD) system to assist radiologists to accurately diagnose Pulmonary Embolism (PE) in CT pulmonary angiography.

Pulmonary embolus is a blood clot, which usually starts from the lower extremity, travels in the bloodstream through the heart and into the lungs, gets lodged in the pulmonary arteries, and subsequently blocks blood flow and oxygen exchange into the lungs. Naturally, based on its relative location in the pulmonary arteries, an embolus may be classified into four groups (central, lobar, segmental and sub-segmental PE). Pulmonary angiography, the gold standard for diagnosing PE, has been rarely used nowadays, as it requires right heart catheterization. Computed tomography pulmonary angiography (CTPA) has become the reference standard modality for PE diagnosis.

Nowadays, pulmonary embolism becomes the third most common cause of death in the US [5]. PE is a common cardiovascular emergency, striking 600,000 Americans each year, causing approximately 200,000 deaths. Most patients who succumb to PE do so within the first few hours following the event. To put this in perspective, Table 1.1 and Fig. 1.1 compare the incidence and mortality of PE with those of breast, colorectal, and lung cancers. A major clinical challenge, particularly in an Emergency Department, is to quickly and correctly diagnose patients with PE and dispatch them to treatment.

Table 1.1: Incidence and mortality of acute pulmonary embolism compared with breast, colorectal, and lung cancers (www.emedicine.com; www.sirweb.org; and www.cancer.gov, NCI estimates for 2008).

	Pulmonary Embolism	Breast	Colorectal	Lung
Incidence	600000	184459	148810	215020
Mortality	200000	40920	49960	161840

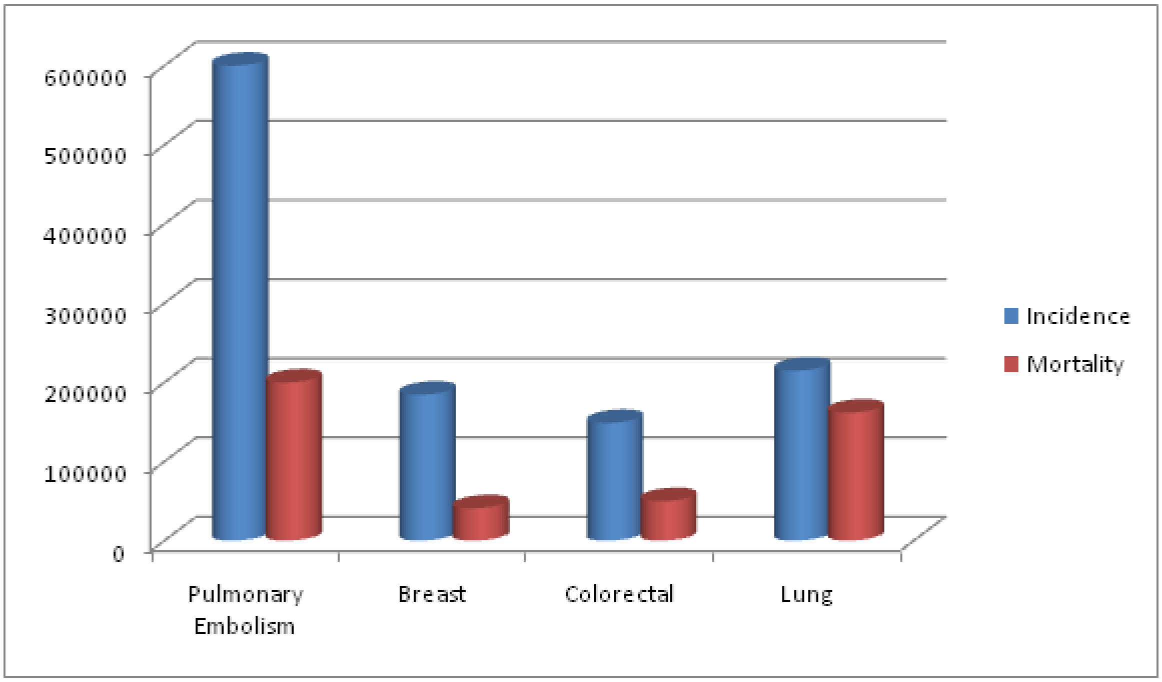

Figure 1.1: Illustration of the incidence and mortality of pulmonary embolism, breast, colorectal, and lung cancers.

1.2 Motivation

To detect PE, especially central PE, we need to identify the pulmonary trunk, shown in Fig. 1.3 (middle). Fig. 1.2 indicates the relationship between central PE and the pulmonary trunk. Detecting the pulmonary trunk can reduce the searching area of central PE among the large volume datasets. One CTPA dataset consists of over 500 individual axial images. The interpretation of these images is complex and time consuming. Moreover, the accuracy and efficiency of interpreting is also

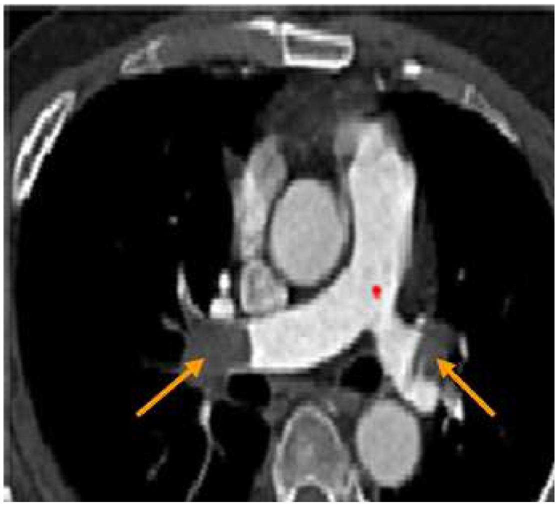

Figure 1.2: Pulmonary trunk (red dot) and central pulmonary embolism (indicated by arrows)

limited by human factors, such as attention span and eye fatigue. Besides, the number of examined patients has increased by an order of magnitude in the past decade, generating enormous CTPA image datasets.

In order to confront this staggering "data explosion" grand challenge, we exploit Boosting based classifier with a large number of image samples, so that the Pulmonary Trunk can be identified without the intervening of human beings. Another advantage of our approach is that no prior anatomy knowledge is required. Therefore, it can be easily adopted to other anatomical structures, such as the carina and the aortic arch, without designing a new framework. The carina and the aortic arch are shown in Fig. 1.3 (left) and (right) respectively. Automatically detecting these anatomical structures, namely the pulmonary trunk, the carina and the aortic arch, is helpful in other image processing applications, such as segmentation, registration, navigation and so on.

1.3 Prototype Structure

In the thesis, we first consider the boosting system under the off-line environment and achieve good performance. However, the off-line environment is not the

Figure 1.3: The carina, the pulmonary trunk, and the aortic arch are shown in left, middle, and right, respectively. The red dots indicate the desired detection positions in the images.

realistic as it requires all the samples to be ready before the training. We thus apply and improve the on-line system, in which samples can be fed into the system one by one instead of in batch.

Our Prototype system combines the off-line and on-line environment together. As shown in Fig. 1.4, users first choose between two options "training a classifier" or "testing the classifier". When choosing to train a classifier, users also need to pick up weather they'd like to generate the model in on-line or off-line environment. If it is off-line training, training samples dataset should be ready and off-line algorithm will be applied. Otherwise, no need to provide the complete training dataset samples to the system at the beginning.

On the other hand, if users select testing processing, they need to feed a trained classifier to the system and apply the classifier onto the dataset where they want to detect the anatomical structures.

1.4 Thesis Organization

The thesis is organized as follows.

In Chapter 2, we review the existing techniques for detecting objects, along with the advantage and disadvantage. The review first discusses high level knowledge based methods and the others before the boosting. And then the

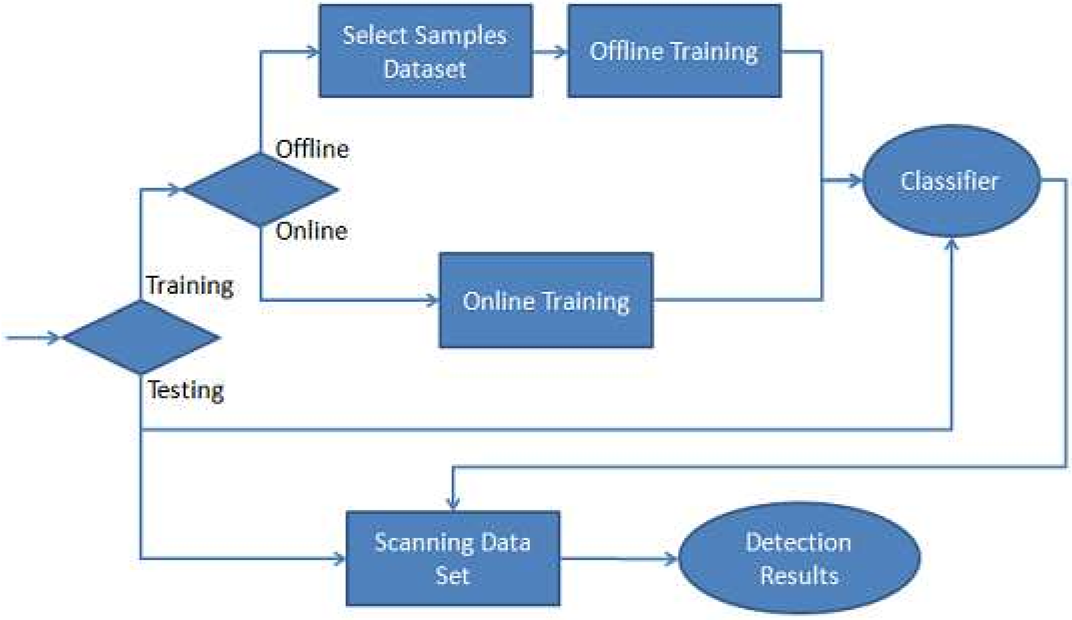

Figure 1.4: Chartflow of the integrated prototype system

classic AdaBoost algorithm and its cascade will be present. We apply another AdaBoost algorithm with a multi-exit cascading scheme and compare the accuracy with the classic algorithm

In Chapter 3, the problem of the off-line AdaBoost will be discussed. To overcome the drawback of the off-line approach, we exploit on-line AdaBoost approach and propose a novel pool based on-line learning framework with improved feature representation.

In Chapter 4, a novel approach which applies asymmetric learning approach is presented. As it can better handle the imbalanced positive and negative samples problem, our new asymmetric approach demonstrates the superiority in term of accuracy over the symmetric AdaBoost approaches.

Chapter 2

OFF-LINE ADABOOST

In this chapter, we first review the different techniques for object detection and then focus on off-line Boosting methods. We present a different cascade scheme on AdaBoost and compare the result with the classic AdaBoost approach.

2.1 Review of the Existed Methods Besides Boosting

Enormous efforts have been put in the research field of detecting object, especially in face detection and anatomical detection in medical images. Among them, a large number of methods more or less apply high level knowledge into the design of their methods.

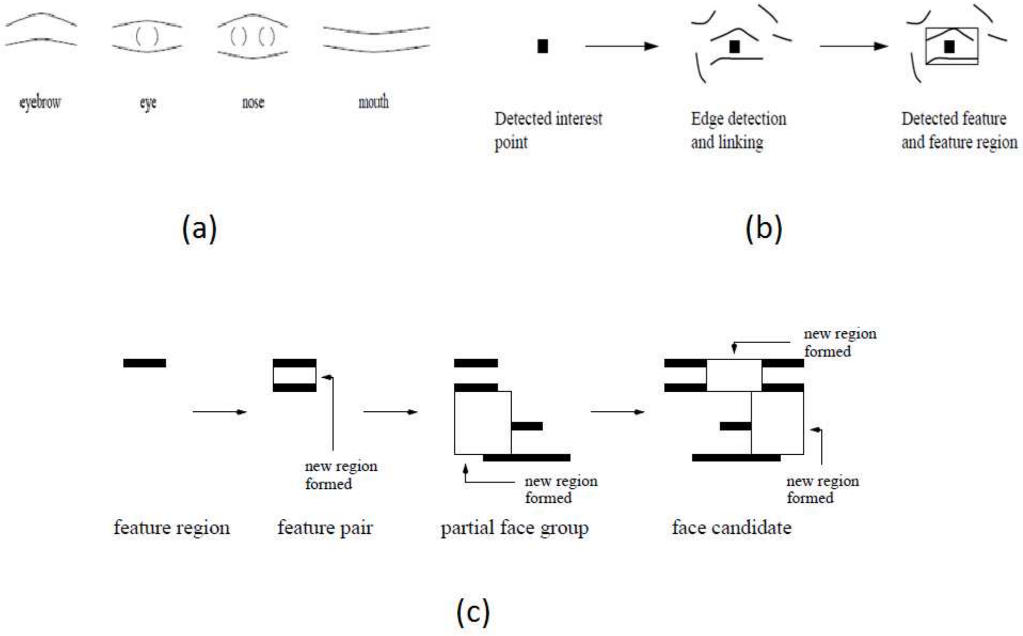

Figure 2.1: (a)Features; (b)Edge detection and linking to a group; (c)Edges groups are merged.

Yow and Cipolla [10] presented a method to detect faces by using edge detection and grouping candidates. Firstly, they selected the interested points based on edge detection. As major edges in faces are horizontal rather than vertical, they combined nearby horizontal edges together and delete short vertical edges. Secondly, edges can be linked and grouped (Fig. 2.1(b)) according to pre-defined features of eyebrow, eye, nose, mouth and so on. Some of the features are shown in Fig. 2.1(a). The grouping of edges is based on the similarity of orientation and strength between the candidate edges and the trained model. Thirdly, groups of edges can be further merged to a bigger group. If the bigger group contains most of the components of faces, it is surely to be a face. The process is illustrated in Fig. 2.1(c). The detection rate in the testing dataset is 85% with 28% false detection rate. And their application is sensitive to the size of the images, which is only good to the image larger than 60-by-60 pixels.

Yang and Huang [11] applied high-level human knowledge about the object to their methods. Their detection rules were built upon their experience. For example, they divided the faces into 20 cells as Fig. 2.2. Rule 1: The center four cells have basically uniform gray level. Rule 2: The upper four cells have basically uniform gray level. Rule 3: The different between center and upper four cells is very significant. Through the mentioned three rules, they can locate faces. Furthermore, they proposed more specific rules for eyes, noses and mouths.

Similarly, Scassellati [12] also used human knowledge in his application. He defined 16 regions and 23 relations for face template, shown in Fig. 2.3. In the testing, the images are tested whether they matched to the templates or not.

Zou [13] first reported their detecting result on the pulmonary trunk. They employs the anatomical knowledge of the lungs and the heart. Anatomically, the aortic arch lies immediately above both the main pulmonary trunk approximately at the same level as the tracheal bifurcation. Computationally, it is easier to detect air within the lumen of the trachea than adjacent vessels in the CTPA images, therefore, they proposed to first identify and trace the trachea beginning at the

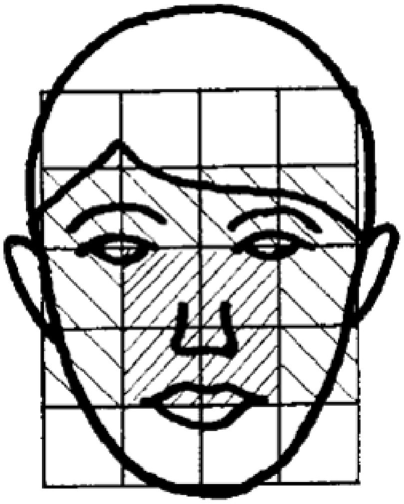

Figure 2.2: Rules of knowledge based method. [11]

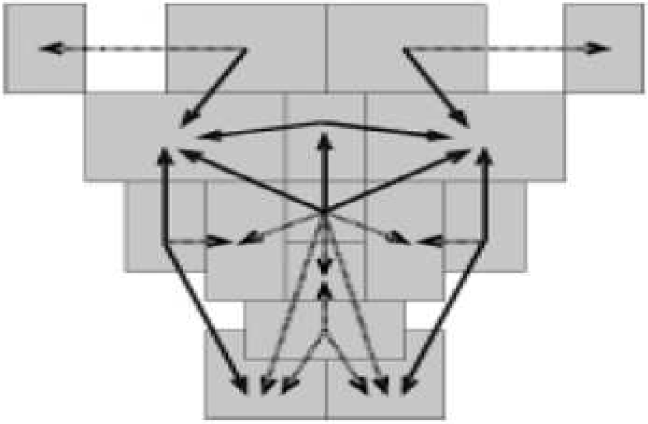

Figure 2.3: A template contains 16 regions (boxes) and 23 relations (arrows) [12]

level of the thoracic inlet inferiorly towards the point of division of the trachea into right and left main bronchi (i.e., the tracheal bifurcation) to facilitate precise and reproducible identification of the aortic arch. Once the aortic arch is localized, the pulmonary trunk can be robustly identified and segmented in a bounding box defined by the aortic arch. Fig. 2.4 demonstrates the process of the detection of the pulmonary trunk. Their evaluation showed that that this anatomy-based approach could correctly detect the pulmonary trunk and provide acceptable segmentation in 60 (about 90%) of 67 cases.

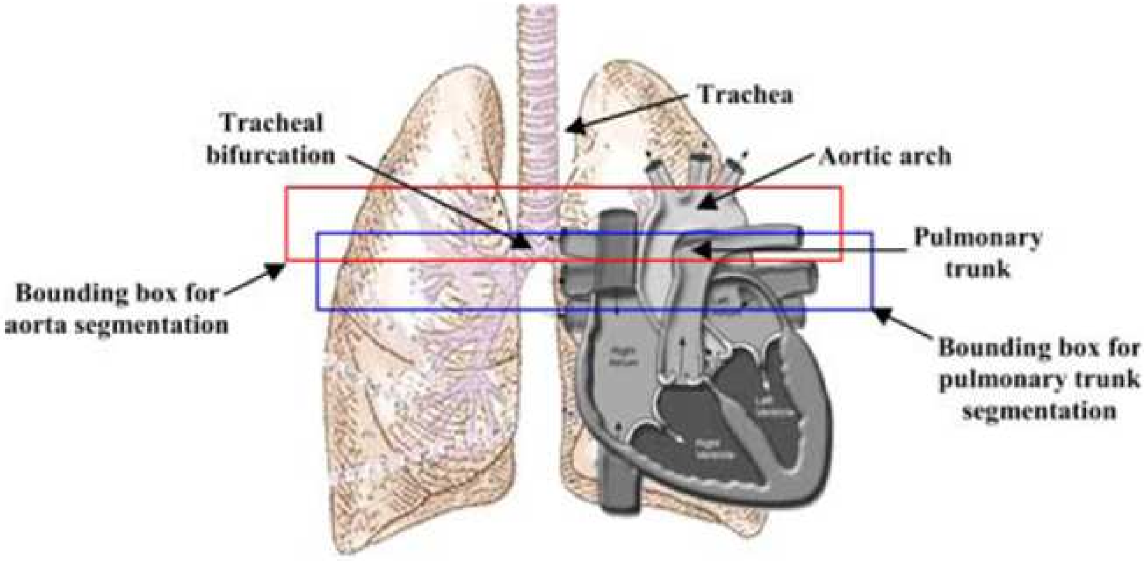

Figure 2.4: Anatomy Based Detection Sequence: (1) Detecting the trachea. (2) Detecting the tracheal bifurcation by tracing airway. (3) Detecting the aortic arch by searching the red bounding box. (4) Detecting the pulmonary trunk by searching the blue bounding box.

The problems of the methods based on high-level human knowledge lie in the bad generalization of the defined rules and templates. It is not easy to include all the details into a unique set and almost impossible to extend to other applications. In most cases, the whole process needs to be redesigned to detect new kinds of objects.

2.2 Review of the Existed Methods

Boosting algorithms have been widely used in machine learning and pattern recognition for object detection. The idea of boosting is to combine weak learners, whose performance is slightly better than 50% (random guess), to form a classifier with high accuracy.

The first real-world application of AdaBoost came from Viola's breakthrough work on face detection [8]. Their learning algorithm, based on AdaBoost, selects the most relevant features from thousands of *Haar features* [14], each corresponding to a weak learner. Their final face detector is a *cascade* of boosted strong classifiers, which is used to scan the images for detecting faces.

Haar Feature and Integral Image

Haar feature (Fig. 2.6) can be defined in terms of several adjacent rectangle regions, which are indicated in white and black. The value of a Haar feature is the sum of the pixels values (intensity) in white rectangle minus the sum of pixel values in the black rectangle. As the length, width, location and the division boundary of the white and black rectangles could vary, one deployment of Haar-like feature pattern could instantiate hundreds of thousands of features.

Haar feature can be computed efficiently by integral image. Integral image is the accumulated summary of the value of pixels. The integral image is built as follows:

$$ii(x, y) = \sum_{x' \leq x, y' \leq y} i(x', y') \tag{2.1}$$

where $ii(x, y)$ is the integral image and $i(x, y)$ is the original image. This can be computed in one pass by

$$s(x, y) = s(x, y - 1) + i(x, y) \tag{2.2}$$

$$ii(x, y) = ii(x - 1, y) + s(x, y) \tag{2.3}$$

where $s(x, -1) = 0$ and $ii(-1, y) = 0$.

The sum of the pixels within rectangle ABCD in Fig. 2.5:

$$\sum_{i(x,y) \in ABCD} = ii(C) + ii(A) - ii(B) - ii(D) \tag{2.4}$$

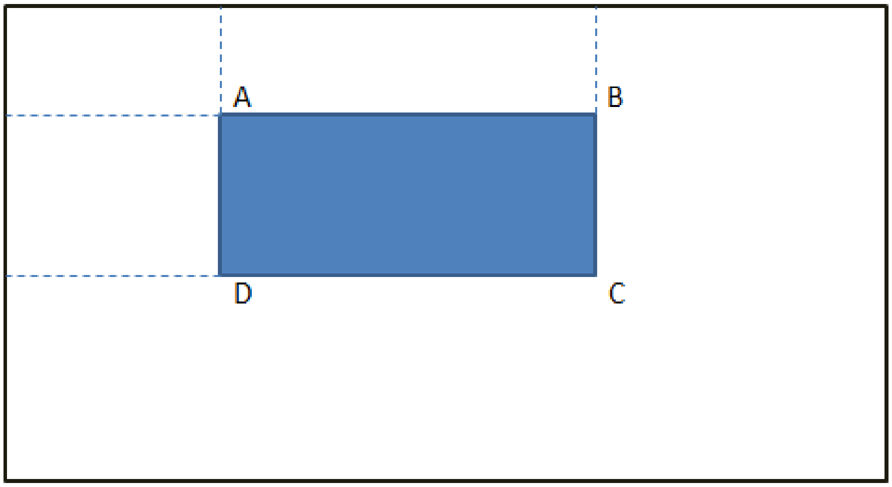

Figure 2.5: Computation of one rectangle in integral image.

To compute the Haar feature rectangles in Fig. 2.6, we just need 6 points in integral image to calculate the sum of pixels in the two rectangles. The time complexity is O(1).

Figure 2.6: Haar feature of two rectangles.

Viola's Cascading Scheme

It is very slow to test all the training samples by using all the weak learner, cascading scheme combines a series of classifiers into a layer to accelerate the object detection process. The idea is to arrange a series of classifiers in a chain or cascade. The cascade chain can reject lots of the negative samples and maintain most of the positive in the early layers. If a candidate is rejected at a layer in the chain, it does not process to the rest of the weak learners in later layers. Clearly, an efficient classifier cascade should reject as many negative candidates as possible, at the earliest layers of the cascade. However, several questions still remain. It is not known how many strong boosted classifiers are needed, how many weak learners each boosted classifier should have, and which combinations of ROC operating points would yield optimal performance.

Viola's AdaBoost [8] uses TPR (True Positive Rate) α_i, FPR (False Positive Rate) β_i and max number of weak learners η_i as the criterion of training a cascade layer. As shown in Fig. 2.7, D_i^+,D_i^- refer to the positive and negative sub-images and their initial weights for training an AdaBoost classifier at layer i. In each layer, during training, more and more weak learners are added to the layer until the target performance (α_i,β_i) or the maximum number of weak learners η_i is reached, after which we start the next layer $i+1$. The output of layer i is a boosted classifier containing all the weak learners from $f_{T_{i-1}+1}$ to f_{T_i}. Upon terminating the current layer, the whole training CTPA datasets are scanned to search for false positives, which will be injected as the new negative samples in the subsequent layer.

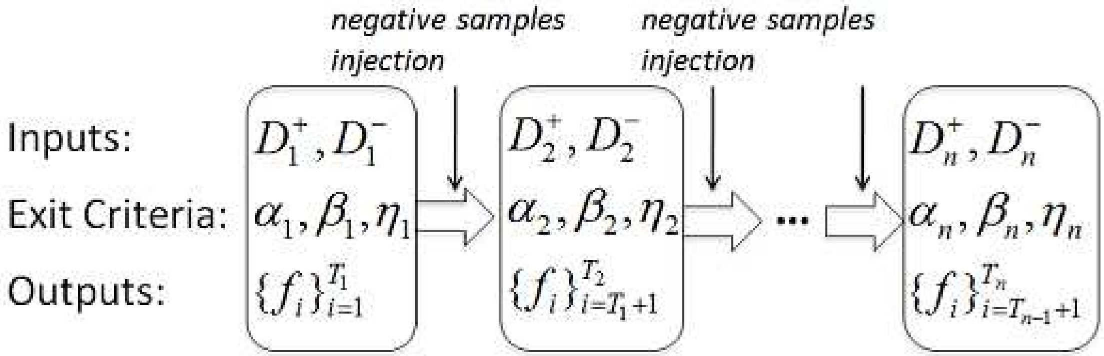

Figure 2.7: Viola's AdaBoost Cascading Scheme.

2.3 Proposed Method: AdaBoost with Multi-exit Cascading Scheme

Viola's cascading scheme does not use any previous weak learners. Instead, We apply multi-exit cascading scheme, which combines the previous weak learners with new trained weak learner. The difference of multi-exit cascading scheme is shown in Fig. 2.8. The output model contains all the weak learners from the very beginning of the whole training process rather than the beginning of the current layer. Multi-exit cascade maintain the previous training information so that it is more stable during the training.

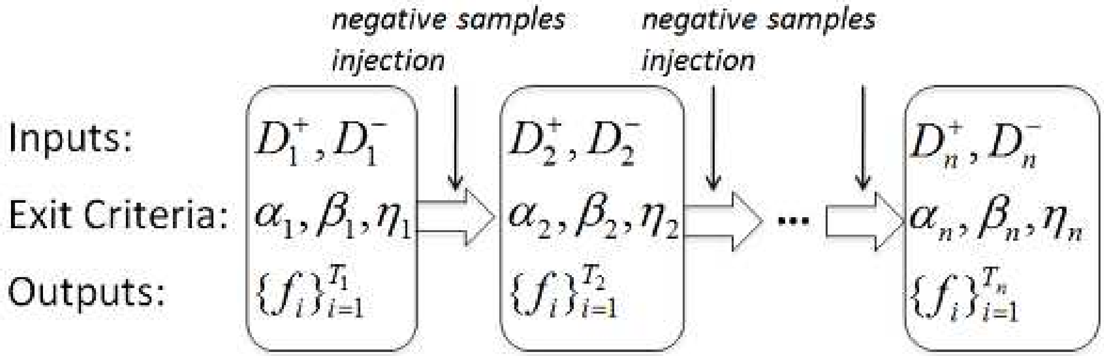

Figure 2.8: Multi-exit Cascading Scheme.

2.4 Experiment and Results

Data Preparation

Our experiments utilize 80 CTPA datasets for training and 77 CTPA datasets for testing. Each dataset contains 450 $\sim$ 600 slices of 512-by-512-pixels. The voxel size of these slices ranges from 0.5 to 0.7 mm in the axial plane, and the slice thickness is 0.5 mm. Every dataset has one and only one pulmonary trunk. The position of a pulmonary trunk is marked by a center point with a bounding box. Positive samples are subimages which contain the desired object, such as the pulmonary trunk. They are obtained by shifting the bounding box 0 $\sim$ 5 pixels, along the x, y, and z axes, and then resized to 25-by-25 pixels. Negative samples are subimages do not have the desired structures. They are randomly selected from the training datasets outside the bounding box of the pulmonary trunk. Examples of positive and negative samples of the pulmonary trunk are shown in Fig. 2.9 and Fig. 2.10. Fig. 2.11 and Fig. 2.12 are some of the positive and negative samples of the carina. Fig. 2.13 and Fig. 2.14 are some of the positive and negative samples of the aortic arch. All the following methods share the same method to obtain positive and negative samples.

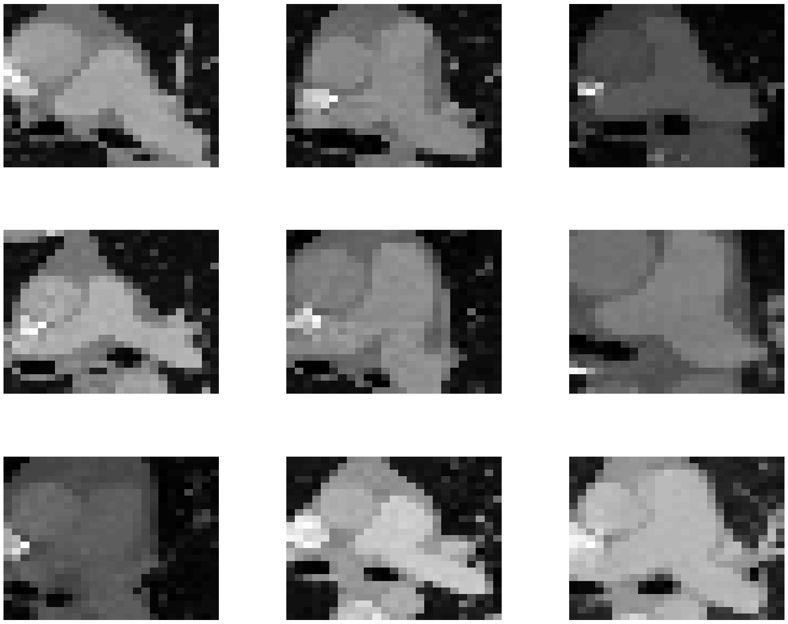

Figure 2.9: Positive Samples of Pulmonary Trunk.

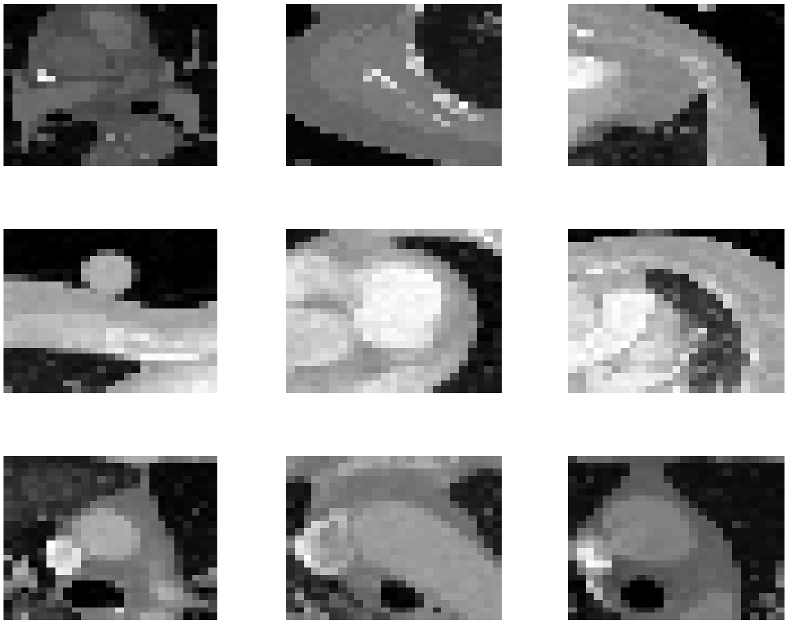

Figure 2.10: Negative Samples of Pulmonary Trunk.

Figure 2.11: Positive Samples of Carina.

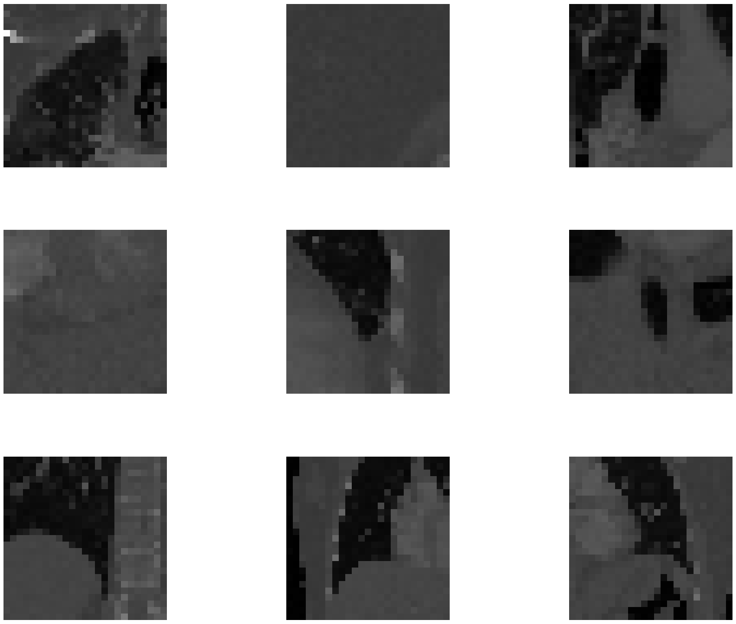

Figure 2.12: Negative Samples of Carina.

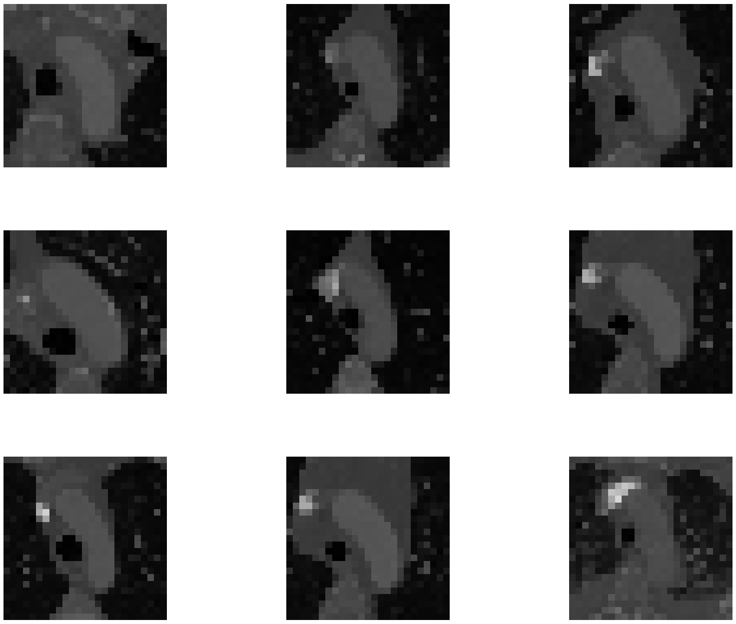

Figure 2.13: Positive Samples of Aortic Arch.

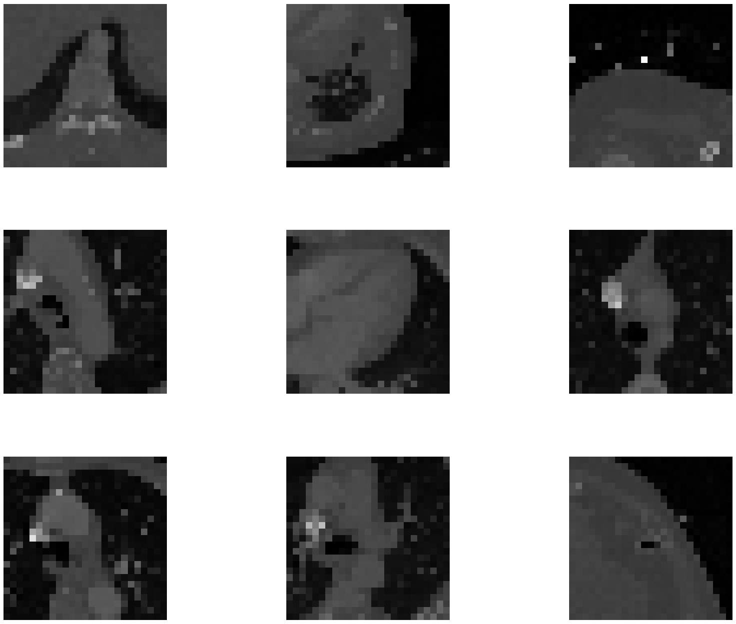

Figure 2.14: Negative Samples of Aortic Arch.

AdaBoost without Cascade

For comparison, 100 positive and 500 negative samples were chosen from each CTPA dataset to train a single AdaBoost. No extra training samples are injected during the training of 100 weak learners. 100% performance can be achieved on the training samples, while only 88.75% detection rate in the training cases and 77.92% in the testing are observed, as shown in.

Viola's AdaBoost Cascading Scheme

For the parameters of Viola's Cascading Scheme, we started off with 100 positive and 100 negative samples from each training case. By negative samples injection between layers, the total number of samples are comparable with the the number of samples in the previous experiment. The training of a cascade layer is terminated when α_i is over 0.99 and β_i is below 0.05 or η_i hits 30. After exiting from one cascade, the program scans the whole CTPA dataset to select at most 100 false positives from each case as the negative samples for the next layer. The number of weak learners from cascade 1 to 6 is 1, 9, 22, 30, 30 and 8. In Fig. 2.15, the accuracy drops and FPR soars when new negative samples are injected. The FPR increases more dramatically in later cascade as the negative samples in that cascade are more similar to the positive and hard to be classified correctly. The accuracy in the detection of the testing cases hits 98.70%, shown in Table 2.1.

Multi-exit AdaBoost Cascading Scheme

We use the same parameters α_i, β_i, η_i as the previous method. The number of weak learners for layer 1 to 7 is 1, 9, 23, 40, 62, 90 and 100, respectively. Fig. 2.16 is the performance trend of multi-exit AdaBoost with cascade. The accuracy in the testing cases reaches 100

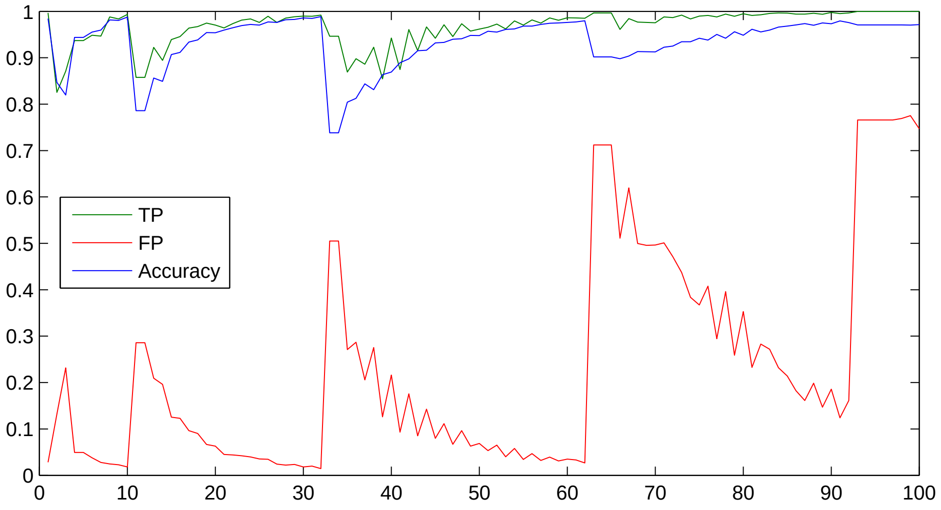

Figure 2.15: The performance of Viola's AdaBoost cascading scheme in training phrase. Layer 1 (weak learner 1); Layer 2 (weak learner 2 - 10); Layer 3 (weak learner 11 - 32); Layer 4 (weak learner 33 - 62); Layer 5 (weak learner 63 - 92); Layer 6 (weak learner 93 - 100).

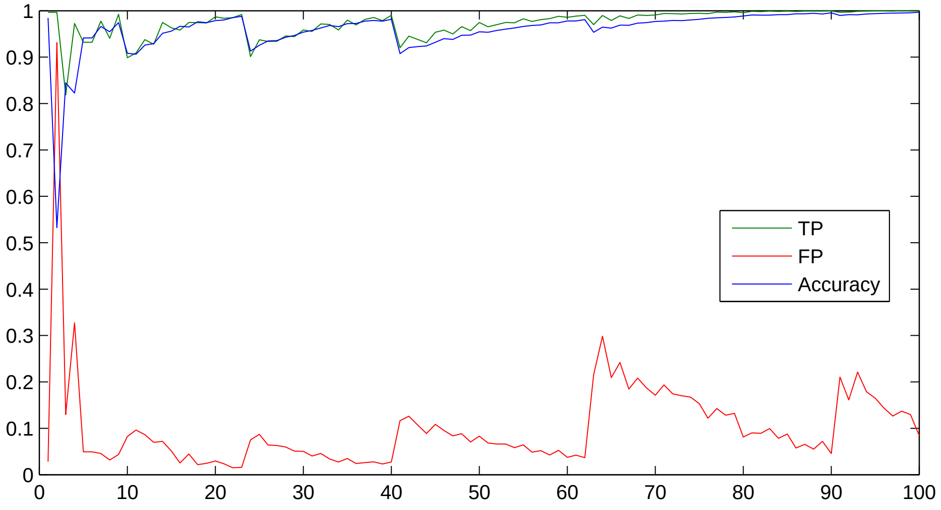

Figure 2.16: The performance of multi-exit AdaBoost cascading scheming in training phrase. Layer 1 (weak learner 1); Layer 2 (weak learner 1 - 10); Layer 3 (weak learner 1 - 23); Layer 4 (weak learner 1 - 40); Layer 5 (weak learner 1 - 62); Layer 6 (weak learner 1 - 90); Layer 7 (weak learner 1 - 100).

AdaBoost with More Representative Negative Samples

To verify the representativeness of the samples and their influence on AdaBoost algorithm, we inject false positive samples collected from the Viola's cascading scheme and multi-exit cascading scheme. The negative sample dataset comsists of all the negative samples injected between cascading layers. The AdaBoost has no cascading scheme but contains more representative negative samples. The accuracy of the detection, shown in Table 2.1, increases significantly from the orignial AdaBoost without cascading schem. Therefore, the quality of the training data (i.e. representativeness of the negative training examples) is one of the utmost important factor for achieving accurate detection.

Table 2.1: Comparison between AdaBoost without cascading, Viola's cascading scheme, Multi-exit cascading scheme and AdaBoost with more representative negative samples.

Methods	Train	Test
AdaBoost without cascading	71/80 (88.75%)	60/77 (77.92%)
AdaBoost with more representative negative samples	77/80 (96.25%)	74/77 (94.10%)
Viola's cascading scheme [8]	80/80 (100%)	76/77 (98.70%)
Multi-exit cascading scheme	79/80 (98.75%)	77/77 (100%)

2.5 Discussion

Besides standard AdaBoost [7, 9] using in Viola's pioneer work [8], other researchers advocated the use of RealBoost [15, 16, 17, 18] and GentleBoost [20]. The concept of AdaBoost, RealBoost and GentleBoost are similar. The key is to select the best weak learner which can separates the positive from the negative. And put more weights on misclassified samples so that the next weak learner will put more emphasis on these samples. However, AdaBoost, RealBoost and GentleBoost apply different algorithms in selecting the best weak learner and updating sample's importance weight.

Table 2.2: Pseudo Code of AdaBoost, RealBoost and GentleBoost

```
Notation:
$I(true) = 1, I(false) = 0$
$\alpha_j$ is the confidence value when $h(x) \in u_j$, where $\sum_j u_j = \mathbb{R}$
Input:
Training example $(x_i, y_i)$; $y_i \in \{+1, -1\}$ for positive and negative examples respectively.
$P$ and $N$ represent the number of positive and negative examples.

Weight Initialization:
$w_{1,i} = \frac{1}{2P}, \frac{1}{2N}$ for $y_i = +1. - 1$ respectively.

for t = 1, ... , T
    1. Normalize examples' weight
        $w_{t,i} = \frac{w_{t,i}}{\sum_i w_{t,i}}$
    2. Select the best feature $h_t(x)$ and its optimal threshold from the feature pool,
    based on the error rate.
        $W_j^+ = \sum_i I(h(x_i) \in u_j) I(y_i = 1) w_i$
        $W_j^- = \sum_i I(h(x_i) \in u_j) I(y_i = -1) w_i$
        2.1 AdaBoost
            $\epsilon = \sum_j min(W_j^+, W_j^-)$
        2.2 RealBoost
            $\epsilon = \sum_j \sqrt{W_j^+ \cdot W_j^-}$
        2.3 GentleBoost
            $\epsilon = \sum_j 2 \cdot \frac{W_j^+ W_j^-}{W_j^+ + W_j^-}$
    3. Calculate the confident value
        3.1 AdaBoost
            $\alpha_{t,j} = \frac{1}{2} \cdot sign(W_j^+ - W_j^-) \cdot ln\frac{1-\epsilon}{\epsilon}$
        3.2 RealBoost
            $\alpha_{t,j} = \frac{1}{2} \cdot ln\frac{W_j^+}{W_j^-}$
        3.3 GentleBoost
            $\alpha_{t,j} = \frac{W_j^+ - W_j^-}{W_j^+ + W_j^-}$
    4. Update examples' weight
        $w_{t+1,i} = w_{t,i} \cdot exp(-|y_i| \cdot \alpha_{t,j})$

The final strong classifier is: $H(x) = sign(\sum_{t=1}^{T} \alpha_{t,j})$
```

Table 2.2 combines AdaBoost, RealBoost and GentleBoost into one pseudocode. The input of the boosting method is the training samples with their labels. After assigned the weights, the total weights of the positive samples should be as same as the weights of the negative samples. The training process is in the loop, in which T is the number of weak learners. Each loop trains one weak learner. Step 1 normalizes the samples' weights.

Step 2 picks up the best feature from the feature pool. The feature domain is separated into several sections. In section j, W_j^+ and W_j^- are the total weight of the positive and negative samples. AdaBoost applies Equation 2.5 to computer ϵ and selects the feature with smallest ϵ.

$$\epsilon = \sum_j min(W_j^+, W_j^-) \tag{2.5}$$

RealBoost uses Equation 2.6. Supposed the feature distribution of positive and negative samples are Gaussian, the overlap of the positive and negative samples should be very small on the feature with lowest ϵ.

$$\epsilon = \sum_j \sqrt{W_j^+ \cdot W_j^-} \tag{2.6}$$

GentleBoost is another variant algorithm which utilizes Equation 2.7 as ϵ.

$$\epsilon = \sum_j 2 \cdot \frac{W_j^+ W_j^-}{W_j^+ + W_j^-} \tag{2.7}$$

Fig. 2.17 compares the relationship between positive weight rates and partition error in AdaBoost, RealBoost and GentleBoost. Positive weight rates are calculated as $\frac{W_j^+}{W_j^+ + W_j^-}$. Partition error is the ϵ value under the relative positive weight rates. If the positive and negative weights are same in a section j, positive weight rates is 0.5 and the partition error should be high. On the other hand, if positive samples dominate the section or have no appearance in the section, the partition error should be closed to zero. All of the three methods follow the above criterion. However, AdaBoost is a linear function. RealBoost and Gentle Boost are smoother when positive weight rates approaches 0.5.

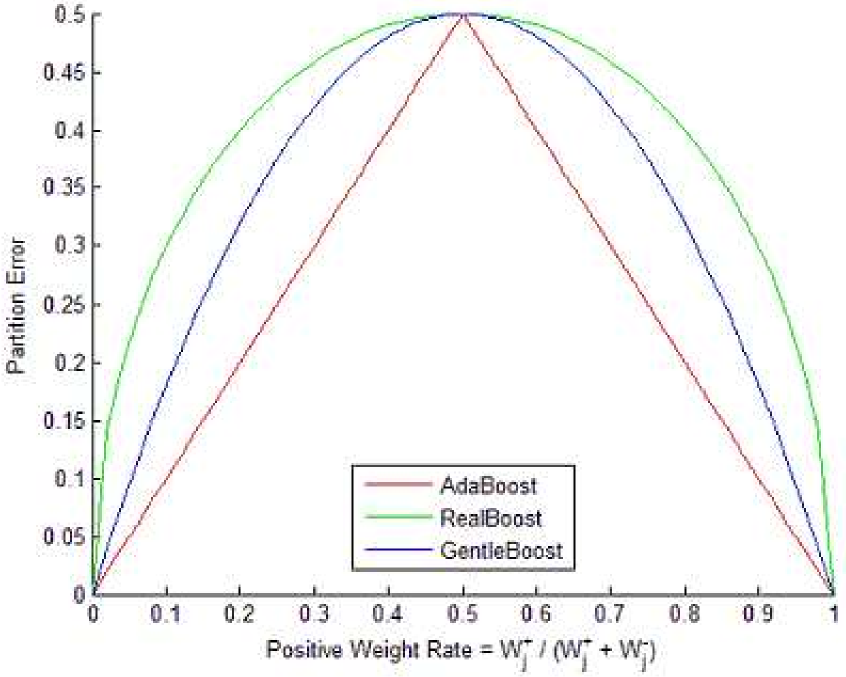

Figure 2.17: Comparison of error computation among AdaBoost, RealBoost and GentleBoost

Step 3 is the other difference in computing the confidence weight among AdaBoost, RealBoost and GentleBoost. The absolute value of confidence should be high when the selected weak learner has low error. The signs of the confidence value indicate weather the sction is classified as the positive or negative. AdaBoost, RealBoost and GentleBoost are applying Equation 2.8, 2.9, 2.10 separately for computing confidence value. Fig. 2.18 analysizes the relationship between positive weight rates and confidence value. AdaBoost and RealBoost share the same curve. However, in AdaBoost, the confidence value is computed on the error rate of the all the sections; in RealBoost, the confidence value is based on one section. Thus, the absolute value of AdaBoost is same for all the section but the sign is different. In RealBoost, different sections can get different confidence value. GentleBoost is a linear function in the computation of confidence value. Another nice property of AdaBoost and RealBoost is that they can reach very high confidence value when the positive weight rate is approaching 0 or 1, but GentleBoost can not.

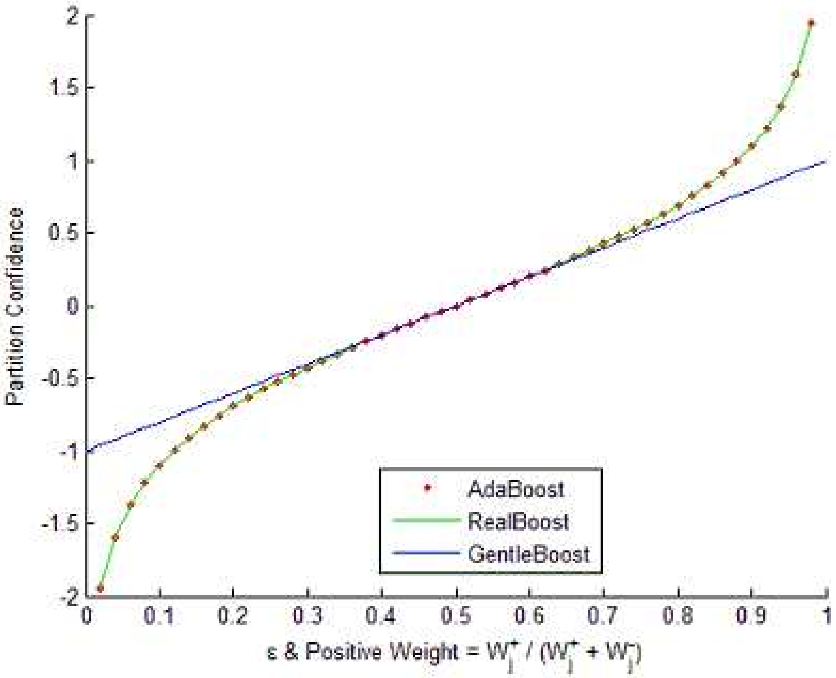

Figure 2.18: Comparison of confidence value computation among AdaBoost, RealBoost and GentleBoost

$$\alpha_j = \frac{1}{2} \cdot sign(W_j^+ - W_j^-) \cdot ln\frac{1-\epsilon}{\epsilon} \tag{2.8}$$

$$\alpha_j = \frac{1}{2} \cdot ln\frac{W_j^+}{W_j^-} \tag{2.9}$$

$$\alpha_j = \frac{W_j^+ - W_j^-}{W_j^+ + W_j^-} \tag{2.10}$$

In step 4, algorithms update training samples' weights to emphasize on the misclassified samples. The weight of correctly classified samples is reduced and incorrectly classified samples is increased. The next weak learner thus pay more attention on the misclassified samples to reduce the error rate.

After obtaining T weak learners, the algorithem applies Equation 2.11 to combine all the weak learner into a strong classifier. The sign of the strong classifier indicates the classified results. $+$ is positive samples and $-$ is negative samples.

$$H(x) = sign(\sum_{t=1}^{T} \alpha_{t,j}) \tag{2.11}$$

There are different opinions on the performance of boosting methods. Lienhart [19] regards RealBoost as the best approach. Brubaker's result [20] demonstrates GentleBoost is superior to other approaches. In the thesis, we adopt AdaBoost for a fair comparison with other methods. Fig. 2.19 illustrates the training process of AdaBoost. In the images, the radius of the samples are responsed to their weight. Large radius means bigger weight and vice versa. The illstration contains two features, representing x axis and y axis respectively. In Fig. 2.19(a), all the positive samples share the same weight and it's same to the negative. In Fig. 2.19(b)-(f), the red dash line is the threshold of the weak learner. "Red" and "Blue" texts beside the threshold indicates the classification results. If the classification is wrong, such as the red samples in the left section of Fig. 2.19(b),the samples becomes larger, which means more weights on this sample. Therefore, the next weak learner, shown in Fig. 2.19(c), tries to classified it correctly.

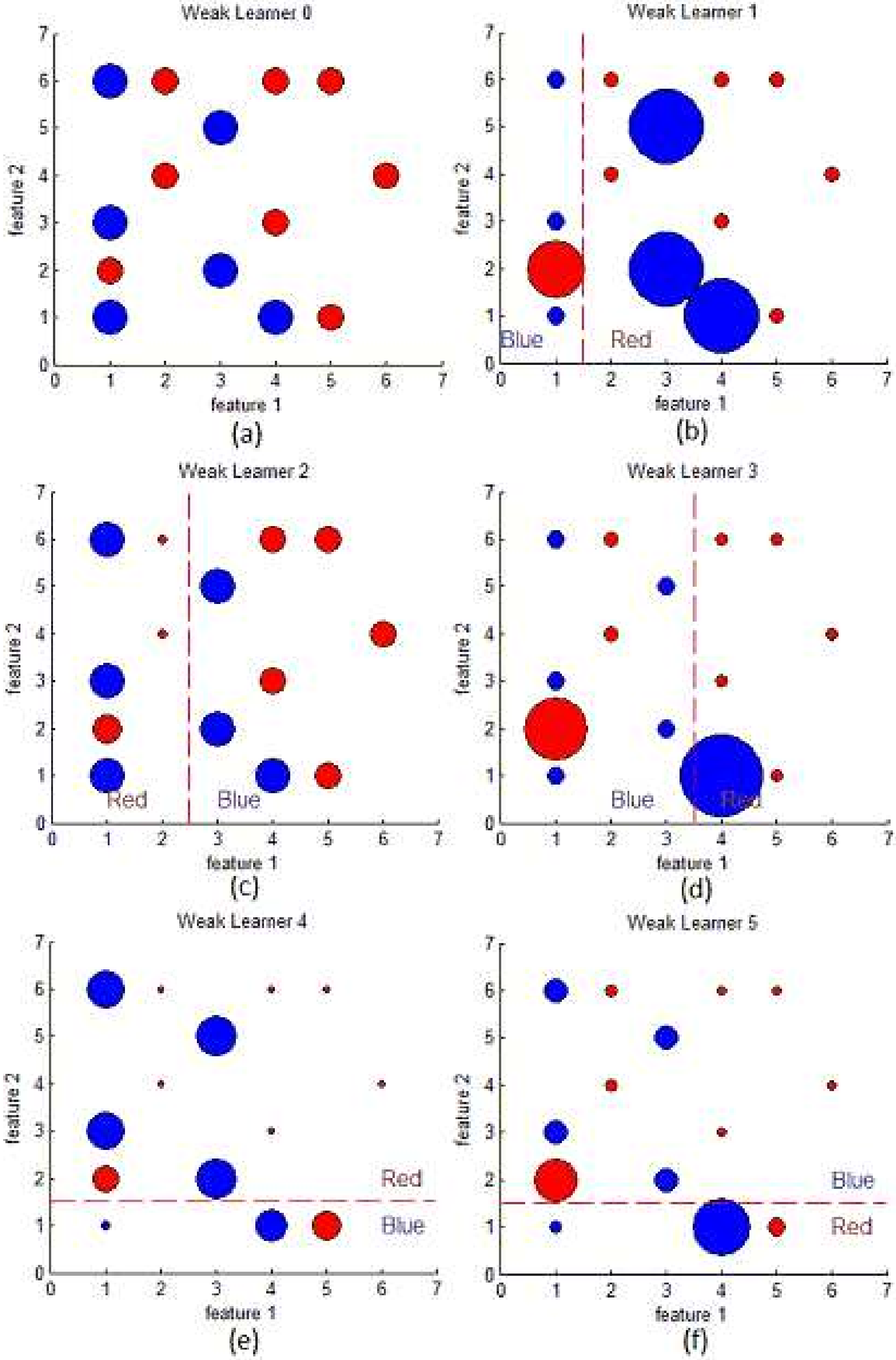

(a) (b) (c) (d) (e) (f)

Figure 2.19: Demonstration of AdaBoost: (a) Original samples. (b)-(f) Samples after reweight based on weak learner 1-5. The radius of the samples are related to their weight. The red dash line is the threshold of the weak learner. One side of the threshold is classified as the red and the other is the blue.

Chapter 3

ON-LINE ADABOOST

Boosting was originally designed for off-line learning. All training samples have to be available prior to the training process. The trained classifier cannot be dynamically adjusted with new coming samples unless retraining from the beginning, which is time consuming and demands to store all the historical samples.

In many applications, particularly in medical image analysis, this is a major drawback as medical data are not generated at one time and retraining is very time consuming with the increasing number of the training samples. To overcome these problems, Oza [28] proposed an on-line boosting method, which could update strong learners without the need for storage of samples and retraining the whole classifier. Grabner and Bischof [6] improved Oza [28]'s work with a selector-based structure, achieving impressive performance in object detection and tracking.

Inspired by the work of Grabner and Bischof [6], we propose a novel on-line learning approach with new weak learner and learning process. The approach eliminates the need of storing historical training samples, and is capable of continuously enhancing its performance with new samples. However, our approach is significantly different from [6] in both the weaker-learner selector and the learning structure. Because of these two novel contributions, our approach outperforms [6] in detecting the three distinct anatomic structures, even achieving a performance comparable to the off-line approaches. Although the performance are compared on three anatomic structures, our approach is generally applicable to a variety of anatomical structures.

3.1 Review of the Existed Methods

As shown in Fig. 3.1, the on-line learning approach proposed in [6] has a layered structure, in which each layer has a number of weak learners (WLs) and associated with one selector. An importance weight λ assigned to each sample. λ is initialized as 1 and updated throughout the layers. The selector chooses the best weak learner based on a performance criterion. Each weak learner corresponds to one feature and is rewarded for correct decision and punished for wrong decision, recorded in λ^{corr} and λ^{wrong}, respectively.

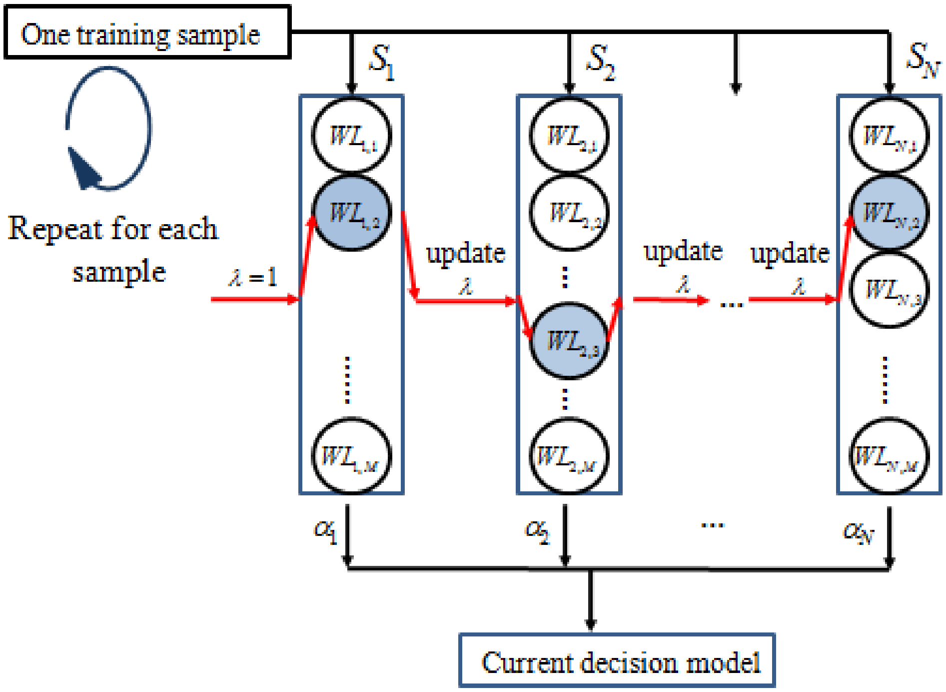

Figure 3.1: Illustration of the layered structure. For each layer, upon arrival of the sample, all the weak learners in that layer are updated and the best one is chosen by the selector. Then, the importance weight of the sample is updated and transmitted to the next layer.

Specifically, in Grabner's [6], each weak learner utilizes two Kalman filters (KF) to perform a binary classification: One for simulating the distribution of positive samples and the other for negative samples. Once a positive (negative) sample x_t arrives at a layer WL_i, the KF associated with the positive (negative) distribution is updated and the threshold θ_i is determined as follows:

$$K_t = \frac{P_{t-1}}{P_{t-1} + R} \tag{3.1}$$

$$\mu_t = K_t \cdot f_i(x) + (1 - K_t) \cdot \mu_{t-1} \tag{3.2}$$

$$P_t = (1 - K_t) \cdot P_{t-1} \tag{3.3}$$

$$\theta_i = \frac{\mu_t^+ + \mu_t^-}{2} \tag{3.4}$$

where P_0, R, and μ are initialized by user, μ_t^+ and μ_t^- are the means of the positive and negative distributions, respectively.

If a weak learner manages to classify the sample into the right category, it will be rewarded. Otherwise, punishment will be assigned. The reward and punishment a WL receives are recorded by μ^{corr} and μ^{wrong}. Equation 3.5 - 3.7 shows how λ can serve as reward or punishment and how it influences ϵ: the error of a weak leaner:

$$K_t = \frac{P_{t-1}}{P_{t-1} + R} \tag{3.5}$$

$$\mu_t = K_t \cdot f_i(x) + (1 - K_t) \cdot \mu_{t-1} \tag{3.6}$$

$$P_t = (1 - K_t) \cdot P_{t-1} \tag{3.7}$$

That is, when a weak learner makes a wrong classification, it is punished by increasing λ^{wrong}. If the classification is correct, it is rewarded by increasing λ^{corr}. Following the same process for each weak learner, selector can obtain the accuracy of all the weak learners and picks up the one with least error rate. Then the voting weight α associated with the best weak learner is computed by the following formula:

$$\alpha = \frac{1}{2} \log \frac{1 - \epsilon}{\epsilon} \tag{3.8}$$

The sample's importance weight λ is also updated and the sample is fed to the next layer. Equation 3.9 provides the updating rule.

$$\lambda = \begin{cases} \lambda \cdot \frac{1}{2 \cdot (1-\epsilon)}, & \text{if } p(x) = y \\ \lambda \cdot \frac{1}{2 \cdot \epsilon}, & \text{if } p(x) \neq y \end{cases} \tag{3.9}$$

Interpreted from Equation 3.9, the importance weight λ decreases when the selector classifies the sample correctly. Otherwise, wrong classification assigns more weights on the misclassified samples in the next layer.

Following this strategy in each layer, selector can obtain the best weak learner and its related voting weight. The final decision model is a linear aggregation of the best weak learners and its voting weight in all the layers. Assume that the model consists of N layers, the strong classifier D is defined as follows:

$$D = sign(\sum_{(} i = 1)^{N} \alpha_i \cdot d_i) \tag{3.10}$$

where d_i is the decision returned by the best weak learner at $i^t h$ layer and takes 1 if the sample contains the desired object otherwise -1. d_i is calculated using the following formula:

$$d_i = sign([f_i - \theta_i] \cdot [\mu^+ - \mu^-]) \tag{3.11}$$

3.2 Proposed method: Pool Based On-line AdaBoost

The proposed approach is an on-line feature selection method. Given a set of training sample, it dynamically updates a pool containing M features and returns a subset of N best features ($N < M$).

To our knowledge, we are the first to address anatomical structure detection with on-line approaches. Other existing approaches are all off-line (e.g., [21, 22, 23, 24, 25]) with focus on detection of other major organs like heart, liver, and spleen.

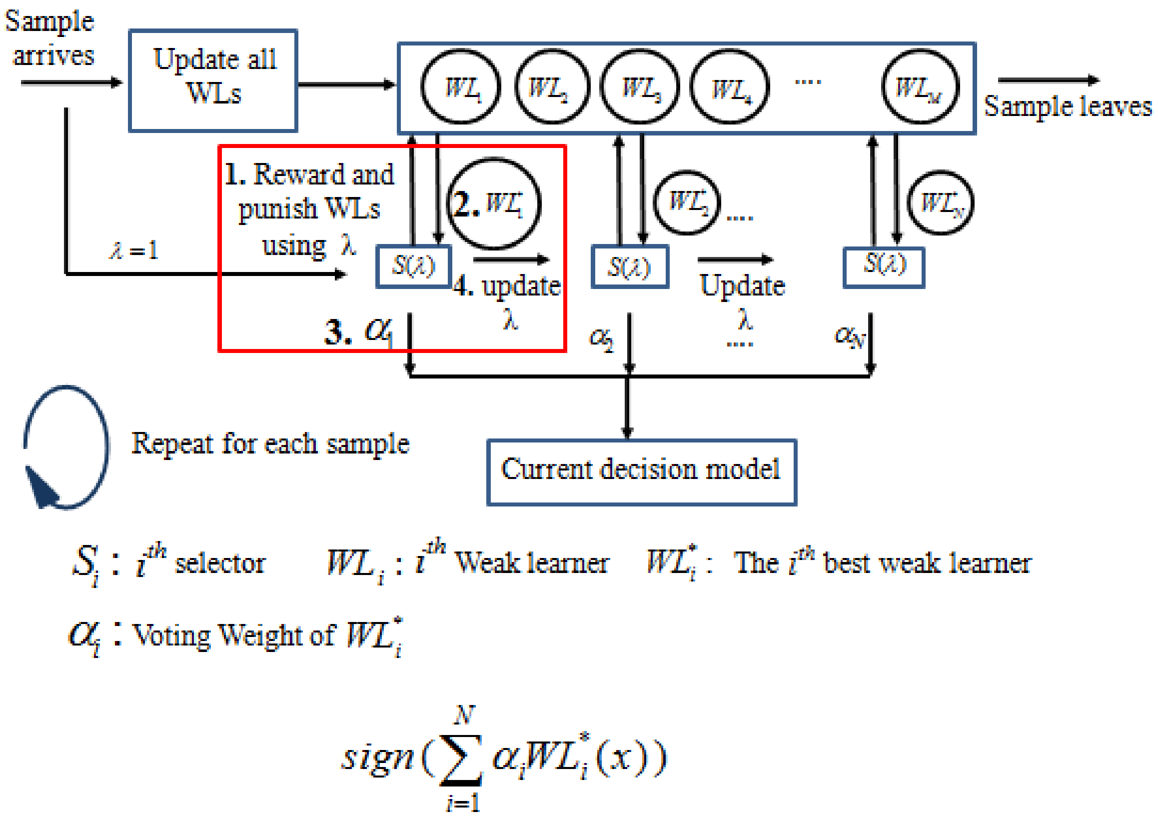

Figure 3.2: Illustration of the proposed pool structure. Four steps are involved in the numeric order. Firstly, punish or reward the entire weak learners in the feature pool. Secondly, choose the best feature from the feature pool as the weak learner. Thirdly, compute the weak learner's voting weight. Finally, update the sample's importance weight and feed it to choose the next weak learner.

Histogram Weak Learner

For each feature in the pool, the corresponded weak learner is comprised of two histograms instead of two Kalman filters, one for positive samples and one for negatives. The two histograms are built as samples come sequentially. In order to continually update the histograms, the range of each feature in the pool must be known in advance. The range of the feature is estimated by examining feature values computed from a temporary set of samples. The approximated ranges are equally divided into 100 bins. Note that, it is likely to encounter training samples whose feature values fall out of the obtained ranges, in that case, they are assigned to the first or last bin depending on weather they are above the maximum or below the minimum. The sample updates all the weak learner's histogram with its sample weight. And then a threshold for each weak learner is chosen to minimize the error.

Learning Process

Table 3.1 is the pseudo code of the proposed on-line AdaBoost. When a sample arrives, all weak learners are updated so as to classify the sample into the right category.

In step one, if a weak learner manages to classify the sample, it will be rewarded by the sample's importance weight λ. λ is high for difficult training samples and low for easy one. If the samples have not been trained, all weak learners are rewarded or punished by $\lambda = 1$. The reward and punishment are recorded by λ^{corr} and λ^{wrong} which are further used to calculate the error rate of each weak learner. Having obtained the error rate of all WLs, selector can choose the best weak learner producing the least error rate.

In step two, the index of selected weak learner is recorded in set A whose members are not considered when choosing the next best weak learner. This prevents the duplicated weak learner in the training process.

In step three, selector computes the voting weight $\alpha_n = \frac{1}{2} ln(\frac{1-error_{m*}}{error_{m*}})$ which indicated the contribution of the weak learner to the final classifier.

In step four, the sample's importance weight is updated. The change of λ reflects the power of the selected best weak learner. If the weak learner has already classified many samples correctly and fails to classify this sample, λ is

Table 3.1: Pseudo code of the proposed on-line learning approach

```
Note: the process is performed for each new sample arriving to the system
Require: training example $(x, y)$, $y \in \{-1, +1\}$
Require: A feature pool containing $M$ features
Require: Total number of weak leaner to be selected $N$ ($N < M$)
Initialization:
    Initialize weak learner: $\lambda_m^{corr}$=1 and $\lambda_m^{wrong}$=1
    Initialize set of selected weak learner: $A = []$
Output:
    Strong classifier: $D(x) = sign(\sum_{i=1}^{N} \alpha_i \cdot WL_i^*(x))$

Update all weak learners
Initialize the importance weight $\lambda$=1
for m = 1,2...,M
   $WL_m$=Update($\lambda$,$WL_m$)
end

Selecting the best N weak learners
for n = 1,2...,N
Step 1: Reward and Punish all M weak learners
   for m = 1,2...,M
      if $WL_m(x)$=$y$
         $\lambda_m^{corr}$=$\lambda_m^{corr}$+$\lambda$     //correct classification
      else
         $\lambda_m^{wrong}$=$\lambda_m^{wrong}$+$\lambda$     //wrong classification
      end
      $error_m$=$\frac{\lambda_m^{wrong}}{\lambda_m^{corr}+\lambda_m^{wrong}}$
   end
Step 2: Select the $n^{th}$ best weak learner
   $m^*$=arg min$_{\{m \notin A\}}$ $error_m$
   Add $m^*$ to set $A$
Step 3: Calculate the voting weight of the $n^{th}$ best weak learner
   $\alpha_n = \frac{1}{2} ln(\frac{1-error_{m^*}}{error_{m^*}})$
Step 4: Update $\lambda$, necessary to choose the next best weak learner
   if $WL_m^*(x)$=$y$
      $\lambda$=$\frac{\lambda}{2(1-error_{m^*})}$     //correct decision
   else
      $\lambda$=$\frac{\lambda}{2(error_{m^*})}$     //wrong decision
   end
end
```

increased dramatically. On the other hand, if the weak learner is known to perform a poor accuracy, it cannot significantly increase λ. The rational behind using and updating λ is to stimulate the next best weak learner to correct the misclassified samples from previous best weak learners.

The output is a strong classifier $D(x) = sign(\sum_{i=1}^{N} \alpha_i \cdot WL_i^*(x))$. If the result is 1, the sample is classified as positive. -1 is the negative samples.

3.3 Experiment and Result

The experiment exploits 157 CT pulmonary angiogram datasets, of which 80 datasets are used for training the decision model and the rest are for testing. Each dataset contains 450 $\sim$ 600 slices. To construct the training samples, 80 training patients are scanned and positive and negative samples of 25x25 pixels are extracted. Because of simplicity and efficiency, Haar features [8] are computed for each 25x25 training sample. Using two Haar patterns of different positions, scales, and aspect ratio, we obtain 101,400 features for each training sample.

Table 3.2 summarizes the detection rates obtained from both off-line and on-line detectors for the training and test patients. the results derived from For our method, we include results deriving from (1) only the novel learning structure as "Proposed + KF" and (2) both the novel learning structure and better weak learner representation as "Proposed + Histogram".

Table 3.2: The detection rates on the pulmonary trunk, the aortic arch and the carina. (Proposed + KF)İ and(Proposed + Histogram) stand for proposed learning structure using Kalman Filter and Histogram as weak learner, respectively.)

Methods	PT[%]		Carina[%]		Aortic Arch[%]	
	Train	Test	Train	Test	Train	Test
Grabner and Bischof [6]	87.5	79.2	98.7	93.4	36.3	47.4
Proposed + Kalman Filter	86.2	88.3	96.2	97.4	63.4	69.7
Proposed + Histogram	95.0	89.6	97.5	98.7	73.8	77.6
Off-line AdaBoost [8]	97.5	93.5	100	100	95.0	93.4

Comparison with Grabner and Bischof [6]: In the case of carina, the proposed method using either Kalman filter or histograms slightly outperforms the Grabner's approach. The small variation in scale and orientation accounts for the high carina detection rates. However, the situation for the pulmonary trunk and aortic arch is quite different. Table 3.2 shows a remarkable drop in the detection rates of both on-line approaches though the proposed method achieves higher performance. Outliers and the wide range of variation in object's scale and orientation decrease the performance and they will be further discussed in the next section.

Comparing to Grabner's approach[6], the performance of the proposed method with pool learner process achieve better performance, explaining the superiority of the proposed learning structure.

3.4 Discussion

This section will further discuss the stability, regarding to outlier. And we will also compare the efficiency and accuracy of Kalman filter and histogram.

Stability

A non-rigid anatomic structure is attributed to human body structures appearing with variation in shape, scale, and orientation from patient to patient. Fig. 3.3 shows four samples for each desired anatomic structures. For each structure, the first two samples stand for the typical shape of the structure while the other samples include notable variation in orientation and shape. As it is seen, while the carina samples exhibit higher level of rigidity, the aortic arch and pulmonary trunk samples display lower rigidity. In this study, the samples which markedly differ in appearance from the typical shape of the structures are referred as positive outliers. Positive outliers affect the learning process and deteriorate the accuracy of the strong weak learner.

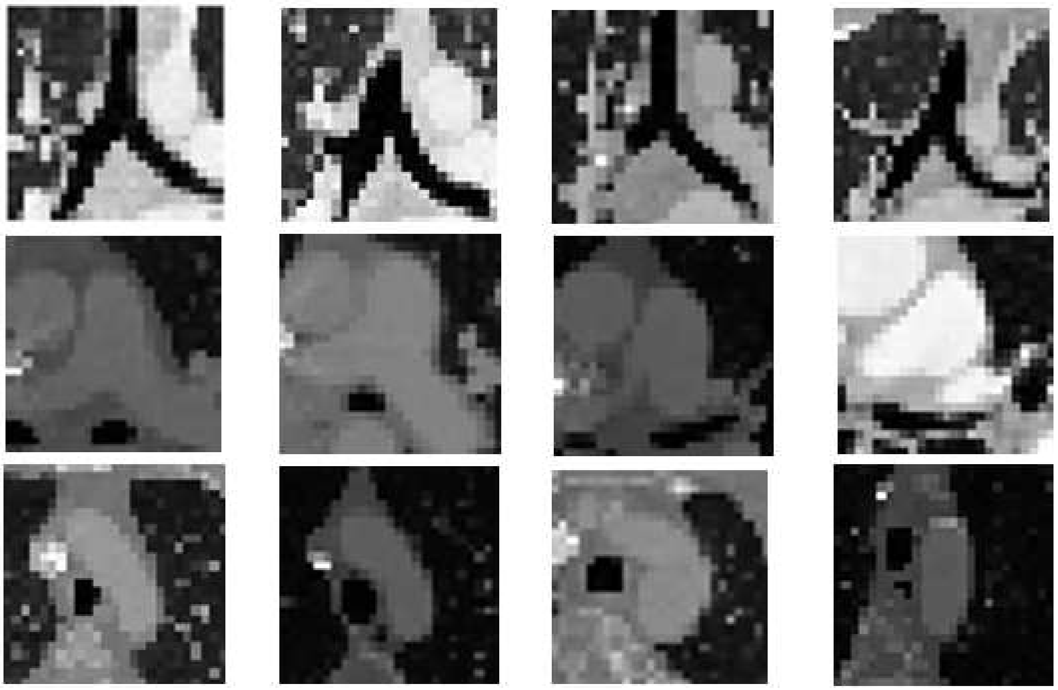

Figure 3.3: The first row contains four carina positive samples, in which the appearance is similar to each other. The second row includes four pulmonary trunk positive samples. The shapes of the third and fourth samples are quite different from the previous two. The third row is for aortic arch, in which the samples are not rotation invariant.

In layered structure, if a positive sample arrives which notably differs in appearance from previous observed positive samples, it will probably be classified as a negative sample (False negative). We regard this sample as positive outlier. Since the best weak learner of the first layer has a very low error rate, the importance weight of the new sample increases significantly (Equation 3.9). The new sample is also likely to be misclassified in the majority of remaining layers, resulting in a large value of importance weight particularly in the late layers of the structure. Fig. 3.4 shows how λ changes for an outlier as it travels through the layers.

Considering the last layer in the layer structure, we can observe a notable drop in the voting weight (Equation 3.8) when the outlier comes to update the weak learner. Before the new sample arrives, weak learners of the last layer were exposed to small and moderate values of λ. However, the coming outlier has a large importance weight λ, changing the balance in favor of λ^wrong, increasing the error of the weak learner and consequently dropping the voting weight. If the decision model is fed a large number of positive outliers, the late layers of on-line learning approach receive very small voting weight, thus minimally contributing to the final decision. Indeed, there is no significant performance improvement as the number of layers exceeds a threshold.

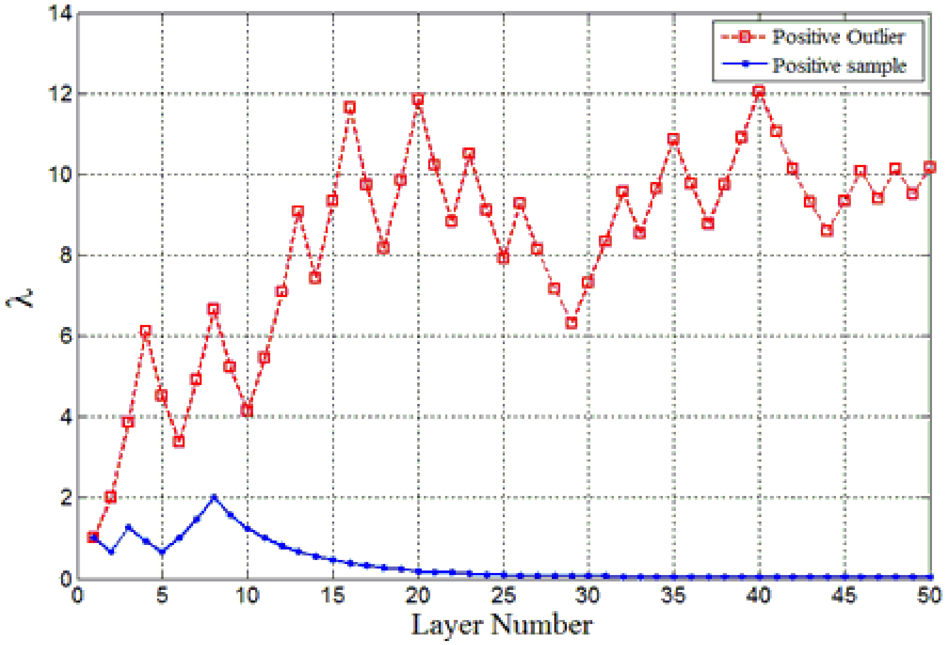

Figure 3.4: The change of λ as a positive outlier (the red curve) and as a normal positive sample (the blue curve). As outliers get a bigger chance to be classified wrong, sample's importance weight λ will be increased dramatically. In later layers, the outlier could dominate the weak learner and hurt the whole strong classifier.

Comparison between Kalman and Histogram

In order to decouple the on-line learning process from the sequence of samples and to include the importance weight in update of each weak learner, we replace the Kalman filter with histograms [26] in the proposed structure.

Histogram fits well to the proposed framework, however; it reduces the efficiency of the original approach. The rationale behind assigning the same subset of WLs to each layer is to update all WLs once when a new sample arrives. It can be realized when we update the decision threshold of each WL irrespective of the importance weight. However, the histogram-based weak learner requires $M \cdot N \cdot NumberOfBins$ operations when updating all the features, increasing the computational time and reducing memory efficiency. $NumberOfBins$ usually is set as 200. On the other side, Kalman filter requires $M \cdot N \cdot 2$ operations.

Chapter 4

ON-LINE ASYMMETRIC ADABOOST

4.1 Review of the Existed Methods

Grabner and Bischof's method [6] is popular in on-line learneing. However, in their implementation, they strictly picked up one positive and four negative samples in each frame and then duplicated positive samples four times to equalize the number of positive and negative samples. In medical image process, the assumption of same number of positive and negative samples is unrealistic. For instance, in each CT pulmonary angiography, there is only one carina, one pulmonary trunk and one aortic arch, which play significant roles in designing a computer-aided diagnosis for detecting pulmonary embolism—one of the most lethal and difficult diagnostic conditions in medicine. As there are far more negative samples than positive in medical image dataset and we do not know the distribution of positive and negative samples, the balanced assumption is not reasonable.

To deal with the imbalanced samples, asymmetric learning was first introduced by Viola and Jones [29]. They developed an asymmetric loss criterion associated with a preset parameter k to penalize k times more on false negative than on false positive. The loss criterion was also adopted in [31]. Pham, et al. [30] utilized two preset parameters, maximum false acceptance rate α_0 and maximum false rejection rate β_0, to setup the asymmetric loss criterion. Pham, et al.'s paper [31] switched their preset parameter to k, which was used in [29]. The existing asymmetric methods require preset parameters; they are not capable of adjusting the asymmetric loss criterion during the training process. There is no general rule for selecting these preset parameters and they have to be chosen based on experience. Different applications may require different parameters.

In medical image analysis, it is not possible to pre-determine the parameters about the skewness of samples. For instance, in the context of anatomical structure detection, we may generate hundreds of distinguished positive samples around the structure of interest (see Fig. 1.3), but there are countless negative samples all over the dataset. Thus, we propose a self-adaptive, asymmetric on-line boosting (SAAOB) method for detecting anatomical structures in CT pulmonary angiography. SAAOB is novel in that it exploits a new asymmetric loss criterion with self-adaptability according to the ratio of exposed positive and negative samples and in that it has an advanced rule to update sample's importance weight taking account of both classification result and sample's label. Validation and comparison are presented based on the experiments to detect the carina, the pulmonary trunk and the aortic arch in both balanced and imbalanced conditions.

The remaining of the chapter is organized as follows. Section 4.2 introduces the methodology and structure of SAAOB, while Section 4.3 presents its performance in both balanced and imbalanced conditions, followed by a discussion in Section 4.4.

4.2 Self-Adaptive Asymmetric On-line Boosting (SAAOB)

SAAOB is an asymmetric version derived from Grabner and Bischof's on-line boosting [6] in which selectors share the same feature pool. This section discusses the contribution, the loss criterion and sample's weight updating rules with the pseudo code of SAAOB (Table 4.1).

Contribution

As the first contribution, we introduce a new asymmetric loss criterion with self adaptability according to the ratio of exposed positive and negative samples. Symmetric on-line learning methods [28, 6] simply update sample's importance weight according to the classification result. In asymmetric on-line learning, it is compelling to update sample's importance weight differently in the situations of true positive, false positive, true negative and false negative.

As our second contribution, SAAOB applies an advanced set of formulas in the four aforementioned situations. As an asymmetric on-line method, SAAOB needs to have different formulas for positive and negative samples. We introduce a set of four different formulas for updating sample's importance weight when the classification is true positive, false positive, true negative and false negative.

The third contribution is the application of SAAOB in the automated detection of anatomical structures. We focus on three anatomical structures, namely, the carina, the pulmonary trunk and the aortic arch (Fig. 1.3) because they provide initial regions of interest for segmentation, and landmarks for registration and navigation. They are particularly important for our current project, requiring extraction of pulmonary artery and airway.

We validate SAAOB from the balanced condition (1 positive: 1 negative) to the extremely imbalanced condition (1 positive: 1000 negative), showing that SAAOB outperforms Grabner and Bischof [6]'s work in imbalanced conditions with slightly better performance in balanced condition.

Asymmetric Loss Criterion

The limitation of on-line boosting methods with symmetric loss criterion [28, 6] arises in the imbalanced conditions in which the number of negative samples is far more than that of positive samples. For example, in the application of detecting anatomical structure, there are at most hundreds of the positive images of the desired structure among millions of the negative images in one patient dataset.

The symmetric loss criterion:

$$\mathcal{E} = \frac{\lambda^{FN}}{\lambda^{TP} + \lambda^{FP} + \lambda^{TN} + \lambda^{FN}} + \frac{\lambda^{FP}}{\lambda^{TP} + \lambda^{FP} + \lambda^{TN} + \lambda^{FN}} \tag{4.1}$$

Table 4.1: Pseudo code of the proposed method: SAAOB

```
Note: the process is performed for each new sample arriving to the system
Require: training example $(x, y)$, $y \in \{-1, +1\}$
Require: weights $\lambda^{TP}_{n,m}$, $\lambda^{FP}_{n,m}$, $\lambda^{TN}_{n,m}$, $\lambda^{FN}_{n,m}$ (initialized with 1)
Require: sample's importance weight $\lambda$ (initialized with 1)
Require: $pos^{num}$ and $neg^{num}$ are the numbers
        of positive and negative samples been exposed to SAAOB (initialized with 1)

for m = 1,2,...,M do // update all the weak learners
    $h^{weak}_m$ = update( $h^{weak}_m$,(x,y))
end for
for n = 1,2,...,N do // update the weak learner parameters in all selectors
    for m = 1,2,...,M do // update the weak learner parameters in selector $n$
        // estimate errors
        if $h^{weak}_{n,m}(x) = +1$ and $y = +1$ then // true positive
            $\lambda^{TP}_{n,m} = \lambda^{TP}_{n,m} + \lambda$
        else if $h^{weak}_{n,m}(x) = +1$ and $y = -1$ then // false positive
            $\lambda^{FP}_{n,m} = \lambda^{FP}_{n,m} + \lambda$
        else if $h^{weak}_{n,m}(x) = -1$ and $y = -1$ then // true negative
            $\lambda^{TN}_{n,m} = \lambda^{TN}_{n,m} + \lambda$
        else if $h^{weak}_{n,m}(x) = -1$ and $y = +1$ then // false negative
            $\lambda^{FN}_{n,m} = \lambda^{FN}_{n,m} + \lambda$
        end if
        // asymmetric loss criterion
        $\mathcal{E}_{n,m} = \frac{1}{1+2\epsilon}[(\frac{neg^{num}}{pos^{num}+neg^{num}} + \epsilon)\frac{\lambda^{FN}_{n,m}}{\lambda^{TP}_{n,m}+\lambda^{FP}_{n,m}+\lambda^{TN}_{n,m}+\lambda^{FN}_{n,m}}$
                $+(\frac{pos^{num}}{pos^{num}+neg^{num}} + \epsilon)\frac{\lambda^{FP}_{n,m}}{\lambda^{TP}_{n,m}+\lambda^{FP}_{n,m}+\lambda^{TN}_{n,m}+\lambda^{FN}_{n,m}}]$
    end for
    // choose the best weak learner and get the parameters for selector $n$
    $m_{best} = argmin_m(e_{n,m}); h^{sel}_n = h^{weak}_{n,m_{best}}; \mathcal{E}_n = \mathcal{E}_{n,m_{best}}; \alpha_n = \log\frac{1-e_n}{e_n}$
    $\lambda^{TP}_n = \lambda^{TP}_{n,m_{best}}; \lambda^{FP}_n = \lambda^{FP}_{n,m_{best}}; \lambda^{TN}_n = \lambda^{TN}_{n,m_{best}}; \lambda^{FN}_n = \lambda^{FN}_{n,m_{best}}$
    //update sample's importance weight
    if $h^{sel}_n(x) = +1$ and $y = +1$ then // true positive
        $\lambda = \frac{1}{2}\lambda\frac{pos^{num}+neg^{num}}{\lambda^{TP}_n+\lambda^{FP}_n+\lambda^{TN}_n+\lambda^{FN}_n}\frac{\lambda^{TP}_n+\lambda^{FP}_n}{\lambda^{TP}_n}$
    else if $h^{sel}_n(x) = +1$ and $y = -1$ then // false positive
        $\lambda = \frac{1}{2}\lambda\frac{pos^{num}+neg^{num}}{\lambda^{TP}_n+\lambda^{FP}_n+\lambda^{TN}_n+\lambda^{FN}_n}\frac{\lambda^{TP}_n+\lambda^{FP}_n}{\lambda^{FP}_n}$
    else if $h^{sel}_n(x) = -1$ and $y = -1$ then // true negative
        $\lambda = \frac{1}{2}\lambda\frac{pos^{num}+neg^{num}}{\lambda^{TP}_n+\lambda^{FP}_n+\lambda^{TN}_n+\lambda^{FN}_n}\frac{\lambda^{TN}_n+\lambda^{FN}_n}{\lambda^{TN}_n}$
    else if $h^{sel}_n(x) = -1$ and $y = +1$ then // false negative
        $\lambda = \frac{1}{2}\lambda\frac{pos^{num}+neg^{num}}{\lambda^{TP}_n+\lambda^{FP}_n+\lambda^{TN}_n+\lambda^{FN}_n}\frac{\lambda^{TN}_n+\lambda^{FN}_n}{\lambda^{FN}_n}$
    end if
end for
$h^{strong}(x) = sign(\sum_{n=1}^{N} \alpha_n h^{sel}_n(x))$ // strong learner
```

equally emphasizes on false negative rate and false positive rate to choose the best weak learner. $\lambda^{TP}, \lambda^{FP}, \lambda^{TN}, \lambda^{FN}$ respectively refer to the true positive, false positive, true negative and false positive weights of a weak learner.

Viola and Jones [29] developed an asymmetric loss criterion for off-line AdaBoost:

$$\mathcal{E} = \sqrt{k}\frac{\lambda^{FN}}{\lambda^{TP} + \lambda^{FP} + \lambda^{TN} + \lambda^{FN}} + \sqrt{\frac{1}{k}}\frac{\lambda^{FP}}{\lambda^{TP} + \lambda^{FP} + \lambda^{TN} + \lambda^{FN}} \tag{4.2}$$

to penalize false negative k times more than false positive. k needs to be known in advance and cannot change during the training. The selection of k is based on designers' experience rather than the skewness of the samples.

We introduce a new asymmetric loss function which can adjust itself during the on-line training:

$$\begin{aligned}\mathcal{E} = \frac{1}{1+2\epsilon}[(&\frac{neg^{num}}{pos^{num} + neg^{num}} + \epsilon)\frac{\lambda^{FN}}{\lambda^{TP} + \lambda^{FP} + \lambda^{TN} + \lambda^{FN}} \\ &+(\frac{pos^{num}}{pos^{num} + neg^{num}} + \epsilon)\frac{\lambda^{FP}}{\lambda^{TP} + \lambda^{FP} + \lambda^{TN} + \lambda^{FN}}]\end{aligned} \tag{4.3}$$

where pos^{num} and neg^{num} are the numbers of positive and negative samples which have been exposed to SAAOB, and ϵ is a smoothing factor. In extremely imbalanced conditions, where $\frac{neg^{num}}{pos^{num}+neg^{num}} \rightarrow 1$ and $\frac{pos^{num}}{pos^{num}+neg^{num}} \rightarrow 0$, the cost of false negative is $\frac{1+\epsilon}{\epsilon}$ times more than the cost of false positive. In balanced condition, when $pos^{num} \approx neg^{num}$, the weights of false negative error and false positive error are same. Naturally, SAAOB outperforms Grabner[6] in imbalanced conditions and should work equally well in balanced condition.

Sample's Importance Weight

Grabner and Bischof [6] updated sample's importance weight with

$$\phi = \begin{cases} \frac{1}{1-\mathcal{E}}, & \text{if } p(x) = y \\ \frac{1}{\mathcal{E}}, & \text{if } p(x) \neq y \end{cases} \tag{4.4}$$

$$\lambda = \frac{1}{2}\lambda\phi \tag{4.5}$$

where x is the sample and y is the label of x. $p(x)$ is the prediction by the classification. This means that their updating rules only depend on the classification result rather than on the sample's label. In asymmetric on-line learning, positive and negative samples must be treated differently. Therefore, it demands different rules for true positive, false positive, true negative, false negative. Considering skewness of samples, classification result and sample's label, we have

$$\varphi = \frac{pos^{num} + neg^{num}}{\lambda^{TP}_{n,m} + \lambda^{FP}_{n,m} + \lambda^{TN}_{n,m} + \lambda^{FN}_{n,m}} \tag{4.6}$$

$$\psi = \begin{cases} \frac{\lambda^{TP}+\lambda^{FP}}{\lambda^{TP}}, & \text{if } p(x) = +1 \text{ and } y = +1 \quad \text{// true positive} \\ \frac{\lambda^{TP}+\lambda^{FP}}{\lambda^{FP}}, & \text{if } p(x) = -1 \text{ and } y = +1 \quad \text{// false positive} \\ \frac{\lambda^{TN}+\lambda^{FN}}{\lambda^{TN}}, & \text{if } p(x) = -1 \text{ and } y = -1 \quad \text{// true negative} \\ \frac{\lambda^{TN}+\lambda^{FN}}{\lambda^{FN}}, & \text{if } p(x) = +1 \text{ and } y = -1 \quad \text{// false positive} \end{cases} \tag{4.7}$$

$$\lambda = \frac{1}{2}\lambda\varphi\psi \tag{4.8}$$

yielding more accurate sample's weight updating in SAAOB.

4.3 Experiments and results

Datasets

The experiments involve in 157 CT pulmonary angiograms datasets, in which 80 datasets are used for training and the rest are for testing. Each dataset contains 450 - 600 512-by-512-pixels slices with 0.5mm×0.5mm to 0.7mm×0.7mm pixel size. The thickness between slices is 0.5 mm. We adopt Wu, et al.'s prototype [27] to generate 4000 positive and 16000 negative 25-by-25-pixels training images from the 80 training datasets for the carina, the pulmonary trunk and the aortic arch separately.

Training Process

Two types of Haar feature patterns [8], horizontal one and vertical one, have been adopted in our experiments, resulting in 101400 Haar features. In the experiments, we uses 50 selectors which share one feature pool with 100 Haar features. The smoothing factor ϵ used in asymmetric loss criterion is set to 0.25. According to equation (4.3), in extreme case, where negative $\gg$ positive, SAAOB at most penalizes 5 times more on false negative than on false positive.

The ratio of positive and negative samples ranges from 1:1 (balanced condition) to 1:1000 (extremely imbalanced condition). We use all 16000 negative samples in the experiment. If the need of positive samples is less than 4000, we randomly select positive samples from the 4000. If the need is more than 4000, we duplicate the positive samples.

Testing Process and Performance Criterion

Detection is based on Viola-Jones' seminal work in face detection [8]. Two levels of testing, sample level and patient level, are conducted in the experiments. At sample level, the trained strong learners are tested on another 25-by-25-pixels image set which also contains 4000 positive samples and 16000 negative samples but all of them are different from the training images. The performance is evaluated by their ROC curves and ROC's AUC (area under curve). At patient level, we applied the strong learners to detect the anatomical structures in 77 testing datasets. If the distance between detection point and ground truth is less than 15 mm, the detection is regarded as correct.

Comparison

Fig. 4.1, Fig. 4.2 and Table 4.2 are the experiment results at sample level. Because of the space limitation, we only include the comparison in aortic arch

Table 4.2: Comparison on AUC between Grabner's symmetric approach[6] and the proposed SAAOB in detecting the pulmonary trunk, the carina and aortic arch.

Apps	Pulmonary Trunk	
Methods	Grabner[6]	SAAOB
1 :1000	0.9352	0.9439
1 :500	0.9458	0.9679
1 :200	0.9513	0.9693
1 :100	0.9516	0.9735
1 :50	0.9613	0.9769
1 :20	0.9716	0.9763
1 :10	0.9774	0.9791
1 :5	0.9824	0.9820
1 :2	0.9863	0.9845
1 :1	0.9867	0.9871
Apps	Carina	
Methods	Grabner[6]	SAAOB
1 :1000	0.9963	0.9949
1 :500	0.9970	0.9953
1 :200	0.9976	0.9974
1 :100	0.9982	0.9983
1 :50	0.9977	0.9988
1 :20	0.9982	0.9990
1 :10	0.9989	0.9993
1 :5	0.9992	0.9992
1 :2	0.9991	0.9992
1 :1	0.9995	0.9997
Apps	Aortic Arch	
Methods	Grabner[6]	SAAOB
1 :1000	0.8873†	0.9503†
1 :500	0.9299	0.9502
1 :200	0.9178	0.9668
1 :100	0.9226†	0.9689†
1 :50	0.9274	0.9741
1 :20	0.9415	0.9760
1 :10	0.9541	0.9789
1 :5	0.9505	0.9803
1 :2	0.9697	0.9789
1 :1	0.9736†	0.9795†

†: Refer to Fig. 4.1 for ROC curves.

‡: The data in the column are also shown in Fig. 4.2.

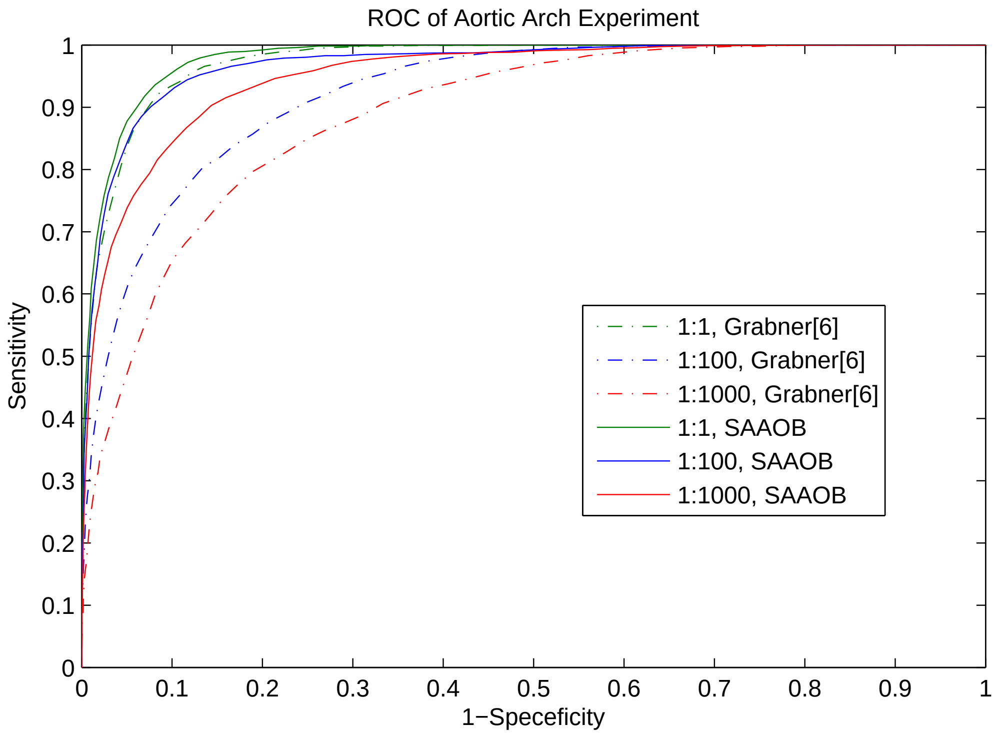

Figure 4.1: The dash-dot lines are the ROC curves by using Grabner[6]. The solid lines are generated by applying SAAOB. From top-left to bottom-right, both ROC curves are in the conditions (positive: negative) 1:1, 1:100 and 1:1000.

detection. Fig. 4.1 are ROC curves and Fig. 4.2 are the changing trend of AUC in Table 4.2. In detecting the aortic arch, SAAOS's performance in harder extreme condition (1 positive: 100 negative) is much better than Grabner[6]'s performance in an easier extreme condition (1 positive: 10 negative) and SAAOS's performance in (1 positive: 100 negative) even approaches to the performance of Grabner[6] in the balanced condition, shown in Fig. 4.1. Table 4.2 also demonstrates the major improvement of SAAOB from Grabner[6] in the pulmonary trunk and the aortic arch detection. Meanwhile, SAAOB also achieves very good performance in detecting the carina as Grabner[6].

Patient level result Table 4.3 indicates consistent results as sample level. SAASO demonstrates much better performance in the imbalanced conditions in detecting the aortic arch and the pulmonary trunk. Because of the smoothing

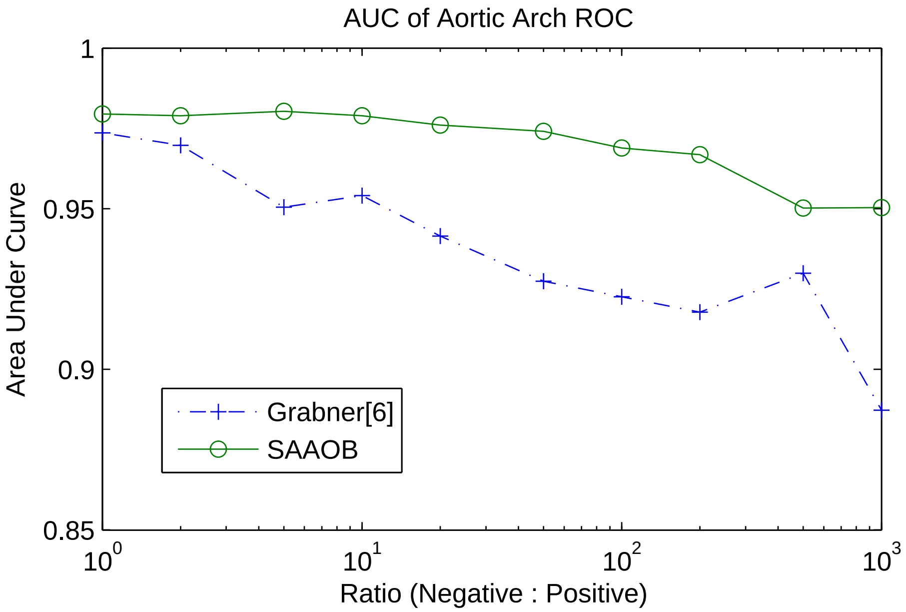

Figure 4.2: The results are from the experiment on the aortic arch. The dash-dot line is the ROC's AUC by using Grabner[6] and the solid line is from SAAOB. The points represent the performance under the ratio (positive: negative) 1:1, 1:2, 1:5, 1:10, 1:20, 1:50, 1:100, 1:200, 1:500 and 1:1000.

factor, SAASO's performance in the balanced condition is as good as or a little better than Grabner[6]'s method. Table 4.3 also shows that SAASO has same good generalization in different applications.

Instead of getting the model by fixing the number of negative samples and reducing the number of positive samples, we fix the number of positive samples and increase the number of negative samples to achieve the imbalanced situation. In Table 4.4, the most imbalanced situation is 1:50 as it may take several months to get all the data in Table 4.3. By comparing Table 4.3 and Table 4.4, we can see that SAASO gets better performance than Grabner[6]'s method in both experiments.

4.4 Discussion

In this Chapter, we propose a new asymmetric loss function with self adaptability and exploit a set of formulas to update sample's weight with classification result and sample's label. Our on-line asymmetric method SAAOB achieves better performance than Grabner [6] in imbalanced conditions. Meanwhile, no need of preset parameters guarantees the stable generalization of SAAOB in all the three anatomical structures detection

The performance of the detection is affected by the hardness of anatomical structures. As the intensity of the carina is much lower than its surroundings, it may be easy to detect the carina. Both SAAOB and Grabner[6] can handle the imbalanced conditions in detecting the carina and achieve good accuracy. Among the three anatomical structures, the carina and the pulmonary trunk have obvious bifurcation structures, which may help them to be detected. 2-D Haar feature was used because of (a) its popularity and efficiency; (b) an unbiased comparison with Grabner's method [6]; (c) our focus on developing a novel learning method rather than designing features. In the future, we will try 3-D Haar features to improve the performance of the classification.

Table 4.3: Comparison of the accuracy in detecting the carina, the pulmonary trunk and aortic arch at patient level between Grabner[6] and SAAOB. The performance is evaluated on both training and testing datasets.

Apps	Pulmonary Trunk [%]			
Methods	Grabner[6]		SAAOB	
	Train	Test	Train	Test
1 :1000	15.00	18.18	40.00	40.26
1 :500	33.75	42.86	72.50	80.52
1 :200	37.50	25.97	61.25	57.14
1 :100	33.75	38.96	65.00	71.43
1 :50	33.75	36.36	51.25	71.43
1 :20	61.25	67.53	68.75	75.32
1 :10	43.75	49.35	53.75	49.35
1 :5	71.25	72.73	72.50	68.83
1 :2	62.50	66.23	75.00	80.52
1 :1	87.50	79.22	81.25	80.52

Apps	Carina [%]			
Methods	Grabner[6]		SAAOB	
	Train	Test	Train	Test
1 :1000	92.41	84.21	86.08	84.21
1 :500	92.41	89.47	89.87	84.21
1 :200	94.94	88.16	94.94	90.79
1 :100	96.20	92.11	94.94	86.84
1 :50	94.94	89.47	96.20	92.11
1 :20	92.41	93.42	93.67	93.42
1 :10	93.67	92.11	96.20	94.74
1 :5	96.20	92.11	94.94	98.68
1 :2	94.94	93.42	93.67	96.05
1 :1	98.73	93.42	96.20	97.37

Apps	Aortic Arch [%]			
Methods	Grabner[6]		SAAOB	
	Train	Test	Train	Test
1 :1000	01.25	05.19	30.00	37.66
1 :500	12.50	12.99	13.75	15.58
1 :200	03.75	07.79	43.75	53.25
1 :100	12.50	07.79	50.00	55.84
1 :50	08.75	18.18	53.75	54.55
1 :20	13.75	12.99	63.75	61.04
1 :10	20.00	23.38	56.25	63.64
1 :5	22.50	19.48	71.25	74.03
1 :2	40.00	25.97	72.50	68.83
1 :1	56.25	57.14	71.25	71.43

Table 4.4: Comparison of the accuracy in detecting the carina, the pulmonary trunk and aortic arch at patient level between Grabner[6] and SAAOB. The performance is evaluated on both training and testing datasets. The model is calculated by incresing the number of negative samples

Apps	Pulmonary Trunk [%]			
Methods	Grabner[6]		SAAOB	
	Train	Test	Train	Test
1 :50	15.00	16.88	75.00	79.22
1 :40	23.75	22.08	50.00	46.75
1 :30	37.50	41.56	82.50	77.92
1 :20	45.00	48.05	77.50	77.92
1 :15	60.00	63.64	77.50	80.52
1 :10	43.75	54.55	78.75	75.32
1 :5	33.75	44.16	70.00	67.53
1 :2	55.00	58.44	76.25	79.22
1 :1	80.00	84.42	78.75	83.12

Apps	Carina [%]			
Methods	Grabner[6]		SAAOB	
	Train	Test	Train	Test
1 :50	93.67	92.11	98.73	98.68
1 :40	86.08	90.79	94.94	97.37
1 :30	98.73	93.42	98.73	97.37
1 :20	98.73	97.37	92.41	96.05
1 :15	91.14	92.11	92.41	94.74
1 :10	94.94	94.74	97.47	93.42
1 :5	91.14	94.74	97.47	90.79
1 :2	94.94	96.05	93.67	97.37
1 :1	97.47	96.05	97.47	92.11

Apps	Aortic Arch [%]			
Methods	Grabner[6]		SAAOB	
	Train	Test	Train	Test
1 :50	06.25	20.78	51.25	57.14
1 :40	12.50	20.78	53.75	42.86
1 :30	13.75	25.97	45.00	48.05
1 :20	08.75	24.68	37.50	33.77
1 :15	11.25	15.58	31.25	48.05
1 :10	17.50	24.68	67.50	61.04
1 :5	42.50	42.86	45.00	44.16
1 :2	31.25	29.87	42.50	44.16
1 :1	38.75	49.35	56.25	61.04

Chapter 5

CONCLUSION

The purpose of the thesis is to detect anatomical structures, including the pulmonary trunk, the carina and the aortic arch. We explore both offline method and online method to achieve the goal. In order to improve the performance, we also deal with the asymmetric learning problems.

In off-line AdaBoost, we review several knowledge based methods and indicate the major problem of these methods are bad generalization. We develop an off-line AdaBoost with multi-exit cascading scheme. The proposed method has been developed to detect the pulmonary trunk, which is opaque to anatomy knowledge of the underlying interesting subjects. The system is insensitive to the position, size and intensity variations of the pulmonary trunk and it can achieve very high accuracy.

The drawbacks of the off-line AdaBoost are presented in Chapter 3. We improved the original on-line method and proposed a new on-line learning framework. The new framework were evaluated on three anatomic structures with different levels of rigidity, demonstrating the proposed method surpasses Grabner's method [6] on the pulmonary trunk and the aortic arch with low level of rigidity. The proposed method also achieves similar performance on the carina which obtains high rigidity. To our knowledge, the presented work is among the first attempts to tackle the anatomic structure detection in on-line learning aspect.

We further proposed a novel asymmetric loss function with self adaptability and exploit a set of formulas to update sample's weight with classification result and sample's label. The proposed online asymmetric method achieved better performance than Grabner's method [6] in imbalanced conditions. Meanwhile, no need of preset parameters guaranteed the stable generalization of SAAOB in all the three anatomical structures detection.

For the future, we plan to

1. extend the 2-D Haar feature into 3-D to capture more distinguishing and representative features for the anatomical structures.
2. apply the algorithm to more anatomical structures, such as the tips of the lung, the ribs or the spine.
3. automatically design the cascade scheme rather than tuning manually.

REFERENCE

[1] Bouma, H. and Sonnemans ,J.J.: Automatic Detection of Pulmonary Embolism in CTA Images. In: IEEE Transactions on Medical Imaging, vol. 28, pp. 1223-1230 (2009)

[2] Zhou, C. and Chan, H.: Automatic Multiscale Enhancement and Segmentation of Pulmonary Vessels in CT Pulmonary Angiography Images for CAD Applications. In: Medical Physics, vol. 34, pp. 4567-4577 (2007)

[3] Liang, J. and Bi, J.: Computer Aided Detection of Pulmonary Embolism with Tobogganing and Mutiple Instance Classification in CT Pulmonary Angiography. In: Information Processing in Medical Imaging, vol. 20, pp. 630-641 (2007)

[4] Dundar, M.M. and Fung, G.: Multiple-instance Learning Algorithms for Computer-aided Detection. In: IEEE Transactions on Bio-Medical Engineering, vol. 55, pp. 1015-1021 (2008)

[5] Rathbun, S. :The Surgeon General’s Call to Action to Prevent Deep Vein Thrombosis and Pulmonary Embolism. In: Circulation, vol. 119, pp. e480-482 (2009)

[6] Grabner, H., Bischof, H.: On-line Boosting and Vision. In: Computer Vision and Pattern Recognition, IEEE Computer Society Conference on, pp. 260–267 (2006)

[7] Freund, Y. and Schapire, R.E.: A Short Introduction to Boosting. In: the Sixteenth International Joint Conference on Artificial Intelligence, pp. 1401-1406 (1999)

[8] Viola, P. and Jones M.: Rapid object detection using a boosted cascade of simple features. In: Computer Vision and Pattern Recognition, pp. 511-518 (2001)

[9] Schapire, R.E. and Singer, Y.: BoosTexter: A Boosting-based System for Text Categorization. In: Machine Learning, 39, pp. 135-168 (2000)

[10] Yow, K.C. and Cipolla, R.: Feature-Based Human Face Detection. In: Image and Vision Computing, vol. 15, no.9, pp. 713-735 (1997)

[11] Yang, G. and Huang, T.S.: Human Face Detection in Complex Background. In: Pattern Recognition, vol. 27, no. 1, pp. 53-63 (1994)

[12] Scassellati, B.: Eye Finding via Face Detection for a Foevated, Active Vision System. In: Proc. of 15th NatŠl Conf. Artificial Intelligence (1998)

[13] Zou X., et al: Anatomy-based Automatic Detection and Segmentation of Major Vessels in Thoracic CTA Images. In: International Journal of Computer Assisted Radiology and Surgery, vol. 2, pp. 68-81 (2007)

[14] Crow, F.C.: Summed-area Tables for Texture Mapping. In: SIGGRAPH Comput. Graph., vol. 18, pp. 207-212 (1984)

[15] Li, S., Zhu, L., Zhang, Z., Blake, A., Zhang, H., and Shum, H.: Statistical learning of multi-view face detection. In: 7th European Conference on Computer Vision, pp. 67-81 (2002)

[16] Bishop, C. and Viola, P.: Learning and vision: Discriminative methods. In: ICCV Course on Learning and Vision (2003)

[17] Wu, B. , Ai, H., Huang, C., and Lao, S.: Fast rotation invariant multi-view face detection based on real adaboost. In: IEEE Automatic Face and Gesture Recognition, pp. 79-84 (2004)

[18] Mita, T., Kaneko, T., and Hori, O.: Joint Haar-like features for face detection. In: ICCV IEEE International Conference on , vol. 2, pp. 1619-1626 (2005)

[19] Lienhart, R., Kuranov, A., and Pisarevsky, V.: Empirical analysis of detection cascades of boosted classifiers for rapid object detection. In: Pattern Recognition, pp. 297-304. (2003)

[20] Brubaker, S.C., Wu, J., Sun, J., Mullin, M.D., and Rehg, J.M.: On the design of cascades of boosted ensembles for face detection. Technical report, Georgia Institute of Technology, GIT-GVU-05-28 (2005)

[21] Zheng, Y., Barbu, A., Georgescu, B., Scheuering, M., and Comaniciu, D.: Fast Automatic Heart Chamber Segmentation from 3D CT Data Using Marginal Space Learning and Steerable Features. In: ICCV , 8 pages (2007)

[22] Liu, D., Zhou, K. S., Bernhardt, D., Comaniciu, D.: Search Strategies for Multiple Landmark Detection by Submodular Maximization. In: CVPR, pp. 2831-2838 (2010)

[23] Zheng, Y., Georgescu, B., Ling, H., Zhou, K. S., Scheuering, M., Comaniciu, D.: Constrained Marginal Space Learning for Efficient 3D Anatomical Structure Detection in Medical Images. In: CVPR , pp.194-201 (2009)

[24] Criminisi, A., Shotton, J., Bucciarelli, S.: Decision Forests with Long-Range Spatial Context for Organ Localization in CT Volumes. In: MICCAI Workshop

on Probabilistic Models for Medical Image Analysis (2009)

[25] Criminisi, A., Shotton, J., Robertson, D., Konukoglu, E.: Regression Forests for Efficient Anatomy Detection and Localization in CT Studies. In MICCAI-MCV Workshop , pp. 106-117 (2010)

[26] Wu, B., Nevatia, R.: Improving part based object detection by unsupervised, online boosting. In: International Conference on Computer Vision and Pattern Recognition, pages 1-8 (2007)

[27] Wu, H., Deng, K., Liang, J.,: Machine Learning based Automatic Detection of Pulmonary Trunk. In: Medical Imaging, SPIE, Vol.7963. (2011)

[28] Oza N.C., Russell, S.: Online Bagging and Boosting. In: Artificial Intelligence and Statistics, pp. 105–112 (2001)

[29] Viola, P., Jones, M.: Fast and robust classification using asymmetric AdaBoost and a detector cascade. In: Advances in Neural Information Processing System, Vol. 14, pp. 1311-1318 (2002)

[30] Pham, M-T, Hoang, V-D.D, Cham T-J: Detection with multi-exit asymmetric boosting. In: Computer Vision and Pattern Recognition, pp. 1-8 (2008)

[31] Pham, M-T, Cham T-J: Online Learning Asymmetric Boosted Classifiers for Object Detection. In: Computer Vision and Pattern Recognition, p. 1 (2007)